2018

STIMULI-RESPONSIVE BIOMATERIALS FOR DRUG DELIVERY TO IMPROVE CANCER IMMUNOTHERAPY AND CHRONIC WOUND HEALING

Anita E. Tolouei
University of Rhode Island, anita.tolouei@gmail.com

STIMULI-RESPONSIVE BIOMATERIALS FOR DRUG DELIVERY TO IMPROVE CANCER IMMUNOTHERAPY AND CHRONIC WOUND HEALING

BY

ANITA E. TOLOUEI

A DISSERTATION SUBMITTED IN PARTIAL FULFILLMENT OF THE REQUIREMENTS FOR THE DEGREE OF

DOCTOR OF PHILOSOPHY

IN

CHEMICAL ENGINEERING

UNIVERSITY OF RHODE ISLAND

2018

DOCTOR OF PHILOSOPHY DISSERTATION

OF

ANITA E. TOLOUEI

APPROVED:

Dissertation Committee:

Major Professor Stephen M. Kennedy

Samantha A. Meenach

Niall J. Howlett

Nasser H. Zawia

DEAN OF THE GRADUATE SCHOOL

UNIVERSITY OF RHODE ISLAND

2018

ABSTRACT

Sequential delivery of biomolecules is very important as many biologics underlying injury and disease follow an orderly and sequenced series of events. Here we developed and introduced for the first time a dual compartment biomaterial system with an outer compartment made of gelatin and inner compartment that is a ferrogel which can be magnetically stimulated in order to provide on-demand, sequential delivery of multiple bio-instructive payload. We studied the potential application of this dual-compartment biomaterial system in different therapeutic contexts that may benefit from on-demand sequential deliveries, such as in cancer immunotherapy and in chronic wound healing.

Chronic wounds can be a result of arrest in the inflammation phase of healing. Although inflammation critically initiates repair and helps clear infections, a prolonged inflammatory reaction can cause considerable harm to the injury site. After an appropriate duration of inflammation, this inflammatory response can be shifted to a more pro-healing response through the delivery of cytokines like interleukin 4 (IL-4) and interleukin 10 (IL-10). These anti-inflammatory cytokines alter the phenotype of macrophages from pro-inflammatory (M1) to anti-inflammatory (M2), suggesting a potentially powerful drug delivery strategy if these cytokines can be delivered in a delayed manner. We hypothesize that the transition of macrophage phenotype from pro-inflammatory (M1) to anti-inflammatory (M2) can be controlled through sequenced delivery of interferon gamma (IFN-γ), followed by IL-4 and/or IL-10. The goal of this research was to develop a wound-healing hydrogel system that initially delivers pro-inflammatory IFN-γ, followed by magnetically triggered delivery of pro-healing (anti-inflammatory) IL-4 and/or IL-10. Our biomaterial system was composed of two-

compartments: (1) a porous gelatin outer compartment designed to recruit macrophages and establish an initial pro-inflammatory (M1) phenotype, and (2) a magnetically responsive alginate inner compartment which was designed to deliver IL-4 and/or IL-10 when magnetically triggered to shift the response to anti-inflammatory by promoting (M2) phenotype. We showed that we can have fast release of IFNg (Promotes M1 phenotype) and MCP-1 (recruits macrophages) initially from the outer compartment while holding on to IL4 and IL10 that is loaded in the ferrogel and have them burst release when applying the magnetic field.

Biomaterial-based cancer immunotherapy strategies require materials capable of recruiting dendritic cells (DCs) and reprogramming them with cancer antigen and danger signal. This strategy requires the implantation of a biomaterial that is loaded with DC recruitment factors, danger signals, and cancer antigen. This co-delivery of danger signal and antigen results in DC activation and homing of cancer-antigen-presenting DCs to the lymph nodes, subsequently triggering an anti-tumor immune response from the host. However, danger signals and antigen diffuse out of the biomaterial while DCs are being actively recruited to the biomaterial. This may result in lower concentrations of these necessary reprogramming agents by the time DCs are recruited and consequently, lower quantities of activated DCs, and a reduced anti-tumor immune response. It is possible that sequential release of DC recruitment and reprogramming factors will enhance the number of reprogrammed DCs over simultaneous release, leading to improved anti-cancer immune responses. In order to test this, a material system with unique delivery capabilities must be developed. Therefore, we designed a biomaterial system capable of first recruiting DCs by initially releasing DC recruitment factors from outer compartment.

This biomaterial can deliver reprogramming agents (i.e., cancer antigen) when magnetically stimulated only after a substantial population of DCs has been recruited. The results showed that we were able to deliver GM-CSF (DC recruitment factor) initially from the outer compartment followed by delivering HSP27 (model cancer antigen) when stimulated in the magnetic field

ACKNOWLEDGMENTS

I would like to thank my advisor Dr. Stephen Kennedy for guiding me through my scientific growth. With his support and granted liberty in conducting my research, I was able to become the scientist I am today. I owe my success to his professionalism, thoughtfulness and kind guidance.

I would also like to thank the University of Rhode Island graduate school and all the faculty and staff professionals in chemical engineering department for providing a great platform for my scientific training. I'd like to express my gratitude to Dr. Samantha Meenach and Dr. Niall Howlett for their insightful participations as my core committee. I would also like to thank my fellow graduate colleagues who helped me in developing ideas and conducting experiments, specially I want to thank Tania Emi for her support. I'd also like to offer a special thanks to Dr. Roxbury and Mitch Gravely who let me do part of my cell culture work in their lab.

I would like to extend special thanks to all the undergraduate students I have had the pleasure of working with: David Edgar, Anne Reisch, Tanner Barnes, Abed Alsasa, Justin Hayes, Sydney Robinson, and Madison West.

Finally, I would like to thank my beloved little sister, Nadia, for being brave for me during past 4 years of living apart. I am also grateful to all my friends specially to my best friend Neda Maddadian who was always there for me and never left my side even though we lived thousands of miles apart. I really appreciate the time I had in Rhode Island and the friendships I built. Above all I want to thank God for giving me strength to always move forward.

DEDICATION

To my parents, Ebrahim and Simin,

For their endless love, encouragement and support

PREFACE

This dissertation is presented in manuscript format in accordance with University of Rhode Island Graduate School Guidelines. There are five chapters included in this dissertation. The first chapter is an introduction and motivation to this work, including a detailing of the problems being address, hypotheses, and goals of the work. The second chapter is review of the literature on Magnetically responsive drug delivery depots as part of an invited review in preparation to be submitted to *Acta Biomaterialia*. The third chapter is published in *Advanced Healthcare Materials* journal with title of "A Magnetically Responsive Biomaterial System for Flexibly Regulating the Duration between Pro- and Anti-Inflammatory Cytokine Deliveries", the Authors are listed in order as Anita E. Tolouei, Nihan Dulger, Rosa Ghatee and Stephen Kennedy. The fourth chapter is a paper in preparation to submit to *ACS Biomaterials Science and Engineering* titled as "Magnetically Responsive Biomaterial System Enables On-demand, Sequential Delivery of Biomolecules for a Variety of Biomedical Applications" and the authors are listed as following Anita E. Tolouei, Tania T. Emi, Zahra M. Madani and Stephen Kennedy. The final chapter is a detailing of the primary conclusions of this dissertation and perspectives on potential next steps in this line of research.

TABLE OF CONTENTS

TABLE OF FIGURES

Chapter 1

Introduction and motivation

Many biological processes that underlie injury and disease can be characterized as highly choreographed sequences of distinct biological events. When aiming to treat injuries and diseases, an overarching strategy is to actively control these sequential biological processes. Local delivery of bioactive molecules can be used to direct individual biological events. Thus, sequences of biological events can be controlled through localized, sequential deliveries of bioactive molecules. While there are previous studies demonstrating sequential delivery of multiple bioactive molecules,[5–7] these studies mainly utilize biomaterials that are preprogrammed to release drug with predetermined temporal profiles. That is, they do not provide real-time control over the timing and sequence of deliveries. Some active materials provide the ability to trigger biomolecular release locally at the implantation site in response to physiological cues such as temperature and/or pH.[8–12] However, these types of active materials often provide slow response times and require stimuli that are not amenable to maintaining in vivo homeostasis (i.e., altering temperature and pH in vivo can be disruptive to biomolecules and tissues and can be difficult to modulate and maintain). Furthermore, clinically, there is need for these deliveries to be adjusted in real time, based on the specifics of each patient and their condition, as well as adjustments needed during the course of treatment

in response to real-time patient diagnosis/prognosis. [4,13] Biomaterials that respond to externally applied cures have been introduced to meet these requirements. For example, biomaterials, studies have shown that materials can be designed to release bioactive payloads in response to external signals such as electric fields[14], optical signals[15], ultrasound[16–18] and magnetic fields[19,20]. Magnetically responsive hydrogels (i.e., ferrogels) are particularly of interest to us because of their biocompatibility, response to benign magnetic signals, and potential flexibility in tuning the timing and rate of the deliveries.[21–23] Ferrogels can be made by mixing iron oxide particles in the gel matrix, allowing the gel structure to deform when exposed to magnetic fields. This deformation results in convective purge of the molecules contained in the gel's matrix.[24–26] Biphasic ferrogels were later developed with macroporous structures for improving the deformation capability of these gels while using a lower concentration of the iron oxide particles. This macroporosity improves biocompatibility of the gel with pore sizes that are significantly enlarged, enhancing molecular and cellular transport through the gel.[27]

While ferrogels have been deployed to provide on-demand, magnetically triggered deliveries, regulation of complex biological processes requires the ability to deliver multiple bioactive compounds from the biomaterial (e.g., cytokines, proteins, etc., often in sequence). Therefore, we developed a dual compartment biomaterial system for delivering critical sequences of bioactive compounds in response to externally applied magnetic signals. This system is composed of an outer compartment in the shape of a hollow cylinder made with porous gelatin and inner compartment which is a cylindrical biphasic ferrogel nestled inside the hollow outer compartment. Each compartment of this system has different design requirements and release mechanisms. The outer

compartment is designed to diffusively release bioactive molecules that are capable of actively recruit a cell type of interest. The inner compartment is designed to harbor a bioactive molecule, only appreciably releasing it to the cells recruited to the outer compartment when instructed to do so in response to an externally applied magnetic gradient. Thus, at its most fundamental, this two-compartment biomaterial system provides a means to sequentially recruit and then modify the behavior of cells after implantation, with real-time control over the timing of this sequence. This ability to flexibly recruit and modify cells to and within a biomaterial structure is of great importance in far-reaching biomedical and clinical scenarios. However, this dissertation will focus on demonstrating sequential biomolecular release in a few contemporary applications: cancer immunotherapy and wound healing (and the associated regulation of the inflammatory response, tissue vascularization, and recruitment and differentiation of tissue specific cell types required for properly regenerating wounds).

1.1 Cancer immunotherapy

Cancer is a group of diseases, which is characterized by abnormal and out of control cell growth caused by mutated DNA and/or environmental effects. In 2016 about 595,690 Americans are expected to die of cancer, or about 1,630 people per day. Cancer is the second most common cause of death in the US and accounts for nearly 1 of every 4 deaths[28]. This emphasizes the necessity of finding new and diverse cancer treatment strategies. One promising cancer treatment strategy is biomaterials-based immunotherapy in which the immune system of a patient's own body is programed in order to initiate an immunological attack against cancer cells [2]. A more traditional (non-biomaterials-based) immunotherapy technique involves monocytes that are extracted from the blood (Fig 1A,

starting at left and moving clockwise to the top) and are differentiated into dendritic cels (DCs) (Fig. 1A, moving from top to right). These immature dendritic cells are then presented with cancer antigens that were extracted from the patient's cancer cells (Fig. 1A, moving from right to bottom). This causes the immature DCs to become mature and active (Fig 1A, bottom). Finally, these activated DCs are re-infused back in to the patient's body (Fig. 1A, moving from bottom to left). In the body, these activated and antigen-presenting DCs travel to the lymph nodes and present those cancer antigens to natural killer cells (T cells). This results in the body mounting an immunological attack against the cancer associated with that antigen.

While yielding some promising results (Fig 1, B, "cell based" survival curve in green, 70% survival in cancer-challenged mice after 90 days), there are some disadvantages to this ex vivo cell-based approach. One is that systemically administered vaccines have short signal duration. Cell-based vaccines they are also very costly and shown limited effectiveness[29]. Furthermore, the vast majority of DCs injected back in to the patient rapidly die and few activated DCs (estimated at only ~0.5-2%) are able to migrate to the lymph nodes which leads to the need for multiple administrations and higher doses. These multiple and higher doses cause systemic toxicity problems in the host [2]. Moreover, this method requires blood withdrawal, DC cell isolation, tumor biopsy, antigen extraction and processing, several DC modifications outside the body, and injecting of DCs back into the body. This, in turn, requires two patient procedures, high cost, and significant regulatory concerns [2]. Because of these disadvantages, indirect cancer immunotherapy vaccines have not been particularly successful into causing solid tumors to regress or increasing patient survival relative to standard treatments [3].

In order to address some of these concerns, biomaterial-based cancer immunotherapy was introduced. In this strategy, an infection-mimicking material is introduced in vivo, providing a site to attract and activate DCs (Fig 1C, i).[2] The biomaterial scaffold is implanted and contains DC recruitment factor, danger signal, and cancer antigen. The recruitment factor releases, forming a gradient, which causes DCs to migrate towards the scaffold (Fig1C, ii). While DCs are in the scaffold, they are subjected to the danger signal and cancer antigen left in the biomaterial (Fig1C, iii). This results in the activation of some of the DCs (Fig1C, iv) and their homing to the lymph node (Fig1C, v). This results in activation of an anti-tumor immunological response from the host. This method leads to promising results. For instance, survival rates in mice that are challenged with melanoma 14 days after drug-loaded biomaterial implantation survive at higher rates (Fig1D, i. blue, red, and dashed black curves) compared to blank biomaterial controls (Fig1D, ii. black curve). Notably, when optimized amounts of GMCSF, danger signal (CpG-ODN), and antigen (tumor lysates) are loaded into these implanted biomaterials, 90% of mice survived after 90 days (Fig1D, i blue curve). However, when the biomaterial was implanted with mice that had existing, well developed 13-day-old tumors, mouse survival rates were less promising (Fig1D, ii).

Even though a better survival rate was observed with loaded biomaterials in comparison to blank biomaterials, double biomaterial implantation only yielded a 20% survival rate after 100 days (Fig3D, ii, comparing the blue curve (Vax,2x) to the black curve (Blank)).

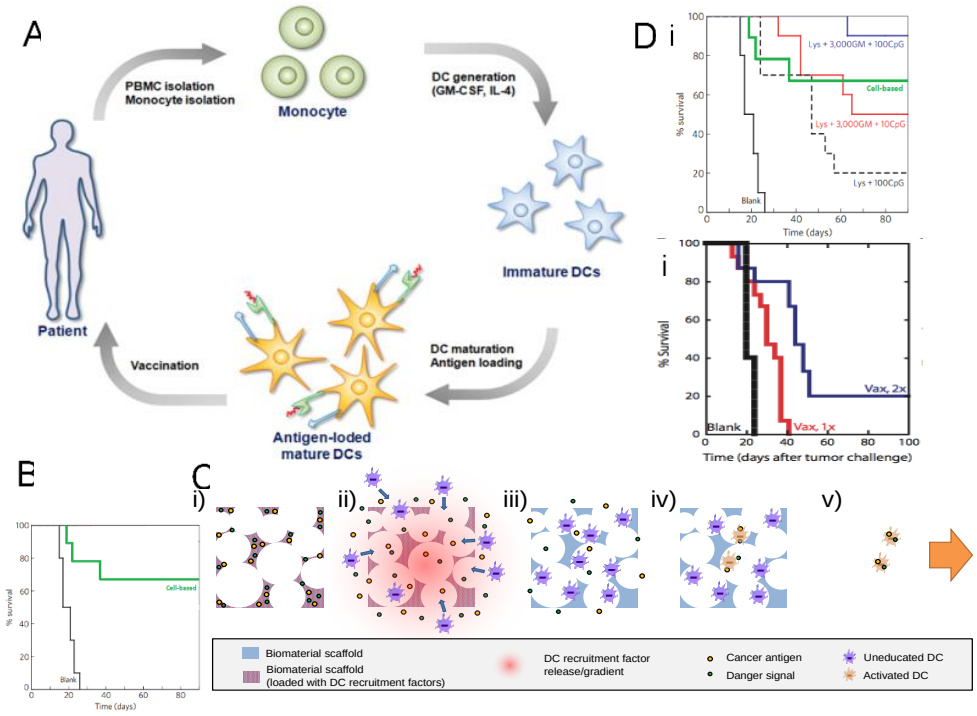

Figure 0.1. Cancer immunotherapy strategies aim to program the body to initiate an anti-tumor response. A. Schematic highlighting the steps involved in indirect cancer immunotherapy. Part A adapted from Kim et al.[1] B. Survival rate for cell-based vaccines (Green) vs. no vaccine (Blank).[2] C. Schematic of biomaterial-based cancer immunotherapy. i. The biomaterial contains DC recruitment factor, danger signal and cancer antigen. ii. Release of DC recruitment factor attracts dendritic cells. iii. While DCs are in the scaffold, they are subjected to the danger signal and cancer antigen left in the biomaterial. iv. This results in the activation of some of the DCs (orange DCs). These activated DCs home to the lymph node. This results in activation of an anti-tumor immunological response from the host. D. Survival rates in an in vivo mouse melanoma model for when: (i) the mouse was implanted with biomaterial 14 days before tumor were introduced to the mouse and (ii) the biomaterial was implanted in mice with already existing (13 days) tumors. Parts B and D(i) adapted from Ali et al.[2]. Part D(ii) adapted from Ali et al.[3]

A potential area for improvement includes fine-tuning the timing and rate of DC recruitment factor, danger signal and antigen presentations. For example, in the Ali et al. system, these three biomolecules begin to diffuse out of the scaffold soon after implantation (Fig. 1,C, ii). Therefore once a robust population of DCs has been recruited

to the scaffold (Fig. 1,C, iii), there are fewer danger signals and antigens left to activate the DCs. This results in even fewer DCs being activated and reporting back to the lymph node (Fig. 1,C, iv and v), and therefore a sub-optimal anti-cancer immunogenic response may occur. Thus if a biomaterial system were capable of initially releasing DC recruitment factors and delaying the presentation of danger signals and antigen molecules, enhanced populations of activated DCs could be generated, resulting in stronger anti-cancer immunological responses. We will therefore aim to develop and test the reprogramming effectiveness of a biomaterial system capable of flexibly controlling the timing and rate of these molecular deliveries in response to externally applied magnetic fields. This biomaterial will result in a high degree of clinical significance by improving cancer survivability and immunity and may be applicable to a wide variety of cancer types. It will also provide a high degree of broad investigative significance by providing a system for examining how the timing and dose of recruitment and reprogramming agents impact immunological responses in general.

The hypothesis guiding this research is that DC activation can be improved by delaying the release of antigens until a vigorous population of DCs has been recruited to the biomaterial. Thus, the overarching aim for this research will be to develop an implantable biomaterial system capable of first releasing DC recruitment factors from its outer compartment, followed by magnetically triggered release of a model antigen. Such

a system may be capable of recruiting DCs and only delivering cancer antigen to recruited DCs at optimized times when stimulated by externally applied magnetic fields.

This proposed biomaterial system consists of two compartments, similarly as described before (Fig. 2A, i and ii). Compartment 1 will initially release DC recruitment factor (GM-CSF) and will have a functionality to maintain recruited DCs (by having a macro-porous structure (Fig. 2A, iii)). This compartment is made from porous gelatin and is loaded with GM-CSF recruitment factor. Compartment 2 consists of a magnetically deformable porous alginate structure that only appreciably releases a model antigen (Heat shock protein 27 (HSP27)) when magnetically stimulated (Fig. 2A, iv and v). This will result in the delivery of antigen in an on-demand, delayed manner. This combined system will be capable of sequentially releasing DC recruitment factors, followed by releasing antigen with magnetic stimuli (Fig.2B). The reason behind choosing these proteins for our work is as follows. The cytokine granulocyte-macrophage colony-stimulating factor (GM-CSF) has been identified as a stimulator of dendritic cell recruitment.[30] Heat shock protein 27 (HSP27) is used as cancer antigen and is often a target for cancer therapy drugs and the immune system. The massive release of HSP due to widespread tumor cell necrosis after cytotoxic drugs can lead to CD8+ T-cell-mediated anti-tumor immune responses.[31] However, for the purposes of this dissertation, HSP27 will be used as a model antigen. Optimizing the effectiveness of cancer antigen is beyond the scope of this work.

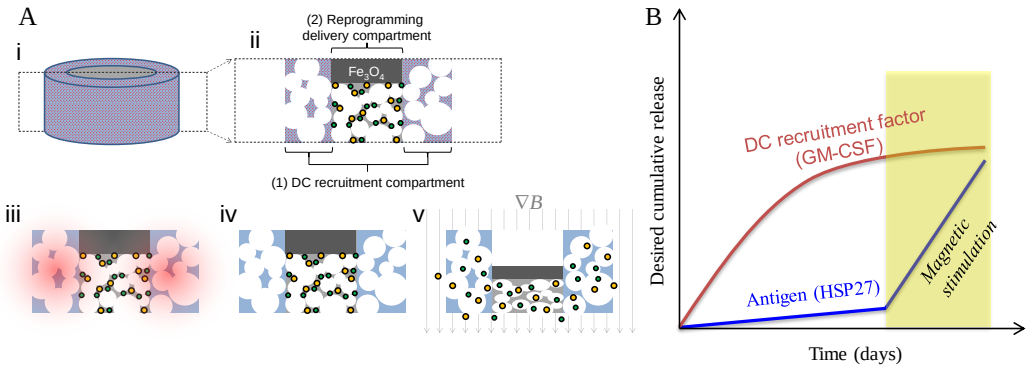

Figure 0.2. Our biomaterial will be designed to initially release DC recruitment factor followed by magnetically triggered release of cancer antigen and danger signal. A. (i-ii) This biomaterial system will be a dual compartment hydrogel composed of a (1) DC recruitment compartment and (2) a magnetically responsive reprogramming delivery compartment. (iii) Compartment 1 initially releases DC recruitment factor (GM-CSF). (iv) While DCs are being recruited, compartment 2 retains antigen (HSP27) and danger signal (single stranded nucleic acids, ssNAs). (v) When magnetically stimulated, compartment 2 releases antigen and danger signal. Part A figure key can be found in Figure 1's caption. B. Desired cumulative release of various molecules from our biomaterial vs. time.

1.2 Chronic wound healing

The proposed two-compartment, magnetically responsive biomaterial system may also be of use in the field of chronic wound healing. In the United States, approximately 6.5 million patients are diagnosed with chronic wounds. The treatment of chronic wounds costs more than $25 billion annually and this is expected to grow due to the increasing cost of healthcare, an aging population, and a rise in the occurrence of diabetes and obesity worldwide.[32] The process of wound healing includes four major steps: hemostasis (blood clothing), inflammation, proliferation, and tissue maturation.[33] Even a slight perturbation in this process can disrupt proper healing, leading to chronic wounds. Chronic wounds are often a result of arrest in the inflammation phase of healing.[33] Although inflammation critically initiates repair and helps clear infections, a prolonged inflammatory reaction can cause considerable harm to the injury site. After an

appropriate duration of inflammation, this inflammatory response can be shifted to a more pro-healing response through the delivery of cytokines like interleukin 4 (IL-4) and interleukin 10 (IL-10). These anti-inflammatory cytokines alter the phenotype of macrophages from pro-inflammatory (M1) to anti-inflammatory (M2), suggesting a potentially powerful drug delivery strategy if these cytokines can be delivered in a delayed manner.

We hypothesized that the two-compartment biomaterial system described above would be capable of (i) initially delivering macrophage recruitment factor and factors that would direct recruited macrophages to adopt a pro-inflammatory M1 phenotype and (ii) magnetically delaying the release of factors that would transition recruited M1 macrophages to anti-inflammatory, pro-healing M2 phenotypes. Specifically, we propose to design the biomaterial system to initially delivery IFN-γ and MCP-1 from the porous outer compartment and retain and magnetically release IL-4 and/or IL-10 from the inner ferrogel compartment. The goal of this research is to develop a wound-healing hydrogel system that allows for the investigation into how the duration of the inflammatory period impacts would healing. Namely, by altering the time at which magnetic stimulation is applied, the proposed biomaterial system will be able to regulate the time point at which the inflammatory response transitions into a pro-healing response. Critically, this is a simple parameter to alter between experiments, enabling rapid investigations into how the timing of these biological processes impact regeneration.

1.3 References

1. Richardson TP, Peters MC, Ennett AB, Mooney DJ. Polymeric system for dual growth factor delivery. *Nat Biotech*. 2001;19(11):1029-1034. http://dx.doi.org/10.1038/nbt1101-1029.
2. Kumar VA, Taylor NL, Shi S, Wickremasinghe NC, D'Souza RN, Hartgerink JD. Self-assembling multidomain peptides tailor biological responses through biphasic release. *Biomaterials*. 2015;52(1):71-78. doi:10.1016/j.biomaterials.2015.01.079
3. Spiller KL, Nassiri S, Witherel CE, et al. Sequential delivery of immunomodulatory cytokines to facilitate the M1-to-M2 transition of macrophages and enhance vascularization of bone scaffolds. *Biomaterials*. 2015;37:194-207. doi:10.1016/j.biomaterials.2014.10.017
4. Priya James H, John R, Alex A, Anoop KR. Smart polymers for the controlled delivery of drugs – a concise overview. *Acta Pharm Sin B*. 2014;4(2):120-127. doi:10.1016/j.apsb.2014.02.005
5. Balamuralidhara V, Pramodkumar TM, srujana N, et al. pH sensitive drug delivery systems: A review. *Am J Drug Discov Dev*. 2011;1(1):28-48. doi:10.39.23/ajdd.2011.24.48
6. Qiu Y, Park K. Environment-sensitive hydrogels for drug delivery. *Adv Drug Deliv Rev*. 2012;64(SUPPL.):49-60. doi:10.1016/j.addr.2012.09.024
7. Chen SC, Wu YC, Mi FL, Lin YH, Yu LC, Sung HW. A novel pH-sensitive hydrogel composed of N,O-carboxymethyl chitosan and alginate cross-linked by genipin for protein drug delivery. *J Control Release*. 2004;96(2):285-300.

doi:10.1016/j.jconrel.2004.02.002

8. Bromberg LE, Ron ES. Temperature-responsive gels and thermogelling polymer matrices for protein and peptide delivery. *Adv Drug Deliv Rev*. 1998;31(3):197-221. doi:10.1016/S0169-409X(97)00121-X

9. Brudno Y, Mooney DJ. On-demand drug delivery from local depots. *J Control Release*. 2015;219:8-17. doi:10.1016/j.jconrel.2015.09.011

10. Farra R, Sheppard NF, Mccabe L, et al. First-in-Human Testing of a Wirelessly Controlled Drug Delivery Microchip First-in-Human Testing of a Wirelessly Controlled Drug Delivery Microchip. 2012;4(122). doi:10.1126/scitranslmed.3003276

11. Kennedy S, Bencherif S, Norton D, Weinstock L, Mehta M, Mooney D. Rapid and Extensive Collapse from Electrically Responsive Macroporous Hydrogels. *Adv Healthc Mater*. 2014;3(4):500-507. doi:10.1002/adhm.201300260

12. Alvarez-Lorenzo C, Bromberg L, Concheiro A. Light-sensitive intelligent drug delivery systems. *Photochem Photobiol*. 2009;85(4):848-860. doi:10.1111/j.1751-1097.2008.00530.x

13. Huebsch N, Kearney CJ, Zhao X, et al. Ultrasound-triggered disruption and self-healing of reversibly cross-linked hydrogels for drug delivery and enhanced chemotherapy. *Proc Natl Acad Sci U S A*. 2014;111(27):9762-9767. doi:10.1073/pnas.1405469111

14. Crasto GJ, Kartner N, Reznik N, et al. Controlled bone formation using ultrasound-triggered release of BMP-2 from liposomes. *J Control Release*. 2016;243:99-108. doi:10.1016/j.jconrel.2016.09.032

15. Lee SF, Zhu XM, Wang YXJ, et al. Ultrasound, pH, and magnetically responsive crown-ether-coated core/shell nanoparticles as drug encapsulation and release systems. *ACS Appl Mater Interfaces*. 2013;5(5):1566-1574. doi:10.1021/am4004705

16. Zhao X, Kim J, Cezar C a., et al. Active scaffolds for on-demand drug and cell delivery. *Proc Natl Acad Sci*. 2011;108(1):67-72. doi:10.1073/pnas.1007862108

17. Hoare T, Santamaria J, Goya GF, et al. A magnetically-triggered composite membrane for on-demand drug delivery. *Nanoletters*. 2011;9(10):3651-3657. doi:10.1021/nl9018935.A

18. Liu TY, Hu SH, Liu KH, Liu DM, Chen SY. Study on controlled drug permeation of magnetic-sensitive ferrogels: Effect of Fe3O4 and PVA. *J Control Release*. 2008;126(3):228-236. doi:10.1016/j.jconrel.2007.12.006

19. Zhang D, Sun P, Li P, et al. A magnetic chitosan hydrogel for sustained and prolonged delivery of Bacillus Calmette-Guérin in the treatment of bladder cancer. *Biomaterials*. 2013;34(38):10258-10266. doi:10.1016/j.biomaterials.2013.09.027

20. Mody P, Hart C, Romano S, et al. Protein-based ferrogels. *J Inorg Biochem*. 2016;159:7-13. doi:10.1016/j.jinorgbio.2016.02.015

21. Cezar C a, Kennedy SM, Mehta M, et al. Biphasic Ferrogels for Triggered Drug and Cell Delivery. *Adv Healthc Mater*. 2014:1-8. doi:10.1002/adhm.201400095

22. American Cancer Society. Cancer Facts & Figures 2016. *Cancer Facts Fig 2016*. 2016:1-9. doi:10.1097/01.NNR.0000289503.22414.79

23. Ali O a, Huebsch N, Cao L, Dranoff G, Mooney DJ. Infection-mimicking materials to program dendritic cells in situ. *Nat Mater*. 2009;8(2):151-158.

doi:10.1038/nmat2357

24. Li WA, Mooney DJ. Materials based tumor immunotherapy vaccines. *Curr Opin Immunol*. 2013;25(2):238-245. doi:10.1016/j.coi.2012.12.008

25. Ali O a, Emerich D, Dranoff G, Mooney DJ. In situ regulation of DC subsets and T cells mediates tumor regression in mice. *Sci Transl Med*. 2009;1(8):8ra19. doi:10.1126/scitranslmed.3000359

26. Kim J, Mooney DJ. In vivo modulation of dendritic cells by engineered materials: Towards new cancer vaccines. *Nano Today*. 2011;6(5):466-477. doi:10.1016/j.nantod.2011.08.005

27. Dranoff G, Jaffee E, Lazenby a, et al. Vaccination with irradiated tumor cells engineered to secrete murine granulocyte-macrophage colony-stimulating factor stimulates potent, specific, and long-lasting anti-tumor immunity. *Proc Natl Acad Sci U S A*. 1993;90(8):3539-3543. doi:10.1073/pnas.90.8.3539

28. Daniels GA, Sanchez-Perez L, Diaz RM, et al. A simple method to cure established tumors by inflammatory killing of normal cells. *Nat Biotech*. 2004;22(9):1125-1132. http://dx.doi.org/10.1038/nbt1007.

29. Sen CK, Gordillo GM, Roy S, et al. Human Skin Wounds: A Major and Snowballing Threat to Public Health and the Economy. *Wound Repair Regen*. 2010;17(6):763-771. doi:10.1111/j.1524-475X.2009.00543.x.Human

30. Frykberg RG, Banks J. Challenges in the Treatment of Chronic Wounds. *Adv Wound Care*. 2015;4(9):560-582. doi:10.1089/wound.2015.0635

Chapter 2

Review of Literature

2.1 Introduction

The ability to produce temporally complex delivery profiles in an on-demand manner is pervasively needed in a wide range of biomedical and clinical scenarios, ranging from cancer treatment to tissue engineering. Stimuli-responsive biomaterials provide a potential means of providing on-demand regulation over temporally complex delivery profiles.[1–4] Some stimuli-responsive materials can be preprogrammed to respond to environmental cues such as pH[5,6] or temperature[7–9] whereas others can be triggered on-demand via externally applied signals. For example, materials can be engineered to release payloads in response to magnetic, electric, ultrasound, and optical signals.[10–13]

The focus of this review is to outline and discuss the potential of magnetically responsive materials for providing on-demand regulation of complex therapeutic delivery profiles. This focus is founded in a number of key factors. First, magnetically responsive biomaterials typically contain magnetic particles[14–16], which are widely used in biomedical applications. For example, magnetic nanoparticles[17,18] and magnetic liposomes[19] can be synthesized and used as drug carriers. The use of iron oxide nanoparticles as magnetic imaging contrast enhancers has made its way to clinical trials[20,21] and are extensively used in magnetic resonance imaging (MRI).[22] Magnetic

particles are also used for targeting purposes[23] and hyperthermia-based treatments (i.e., cancer treatment involving heating up the cancer cells to temperature between 43°C to 46°C when cell viability drops and becomes more vulnerable to chemotherapy and radiation). [24–26] Furthermore, magnetic fields similar to those used in these treatments are widely used in everyday scenarios (e.g., at airport security, at store exits, in MRIs, and even in some children toys) and have been demonstrated to be harmless to the human body.[22,27] Taken altogether, this well-established track record of using magnetic particles and magnetic field stimulation creates a strong precedence for their diagnostic and therapeutic use. This suggests that magnetic nanoparticle integration into drug delivery systems and remote stimulation using magnetic fields may be a viable option for achieving on-demand control over biomolecular deliveries.

This review will concentrate on hydrogel-based drug delivery systems that are integrated with magnetic particles, endowing them with on-demand delivery capabilities when subjected to remotely applied magnetic fields. Hydrogels are used significantly in drug delivery applications due to a number of desirable features.[28,29] For example, they can absorb water up to 30% of their dry weight and can be made from biocompatible polymers. They can also be chemically and mechanically modified to better interface with tissues.[30–33] Ferrogels are hydrogels that have been integrated with iron oxide particles in their polymeric network and their preparation method is very well established.[34–36] Here, we will categorize the drug release mechanisms from ferrogels and will discuss the tunable parameters effecting each release mechanism. This, in turn, may shed light on how magnetically responsive ferrogels can be designed to achieve magnetic control over more temporally complex drug delivery profiles. We will then proceed to

highlight the importance of producing multi-drug release profiles in an on-demand manner and underscore the limited amount of work being done in this area.

2.2 Magnetically triggered release mechanisms

2.2.1 Inductive heating, agitation, or melting of polymer structures

Hydrogels can be designed to change phase (e.g., collapse, degrade, or swell) when inductively heated or agitated under magnetic stimulation, leading to release of payloads.[37–39] The super paramagnetic iron oxide nanoparticles (SPIONs) inside these hydrogels can absorb energy from high-frequency magnetic fields, which in turn leads to swelling or collapse of the hydrogel matrix due to changes in temperature. This inductive heating occurs when an alternating magnetic field (AMF) is applied to SPIONs. Heat is generated due to Neel and Brownian relaxation phenomena.[40,41] This energy then transfers to the hydrogel's polymer matrix which can lead to conformational changes such as polymer collapse or degradation (Figure 1).[42] In a study by Hu et al.,[43] the authors were able to show the pulsatile delivery of vitamin B_{12} loaded in the polymeric system. This system was made by embedding iron oxide nanomagnets with average diameter of 40 nm within gelatin polymer network crosslinked with genipin. When a high frequency magnetic field was applied, the nanoparticles twisted and shaken, causing the polymeric network to decompose and release its content. Vibrations of the particles were also shown to increase the local temperature of hydrogel as well, which could potentially be problematic if this system were used for delivering more sensitive molecules such as proteins (which can denature at higher temperatures, rendering them bio-inactive).

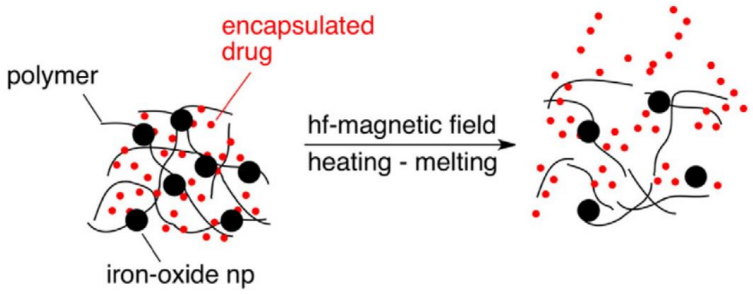

Figure 0.1. Schematic of heat-inductive release mechanism from hydrogels triggered with magnetic field. Figure copied from Brundo et al.[44]

There are several other notable examples of hydrogel systems that exploit inductive heating/agitation from magnetic fields to externally regulate drug delivery profiles from hydrogel systems. For example, N-isopropylacrylamide (NIPAAm) is a temperature responsive polymer with a lower critical transition temperature (LCST) between 30 and 35°C.[45] In one study, NIPAAm gels were made in disk shapes (15 mm diameter and 0.5 mm thickness) and iron oxide nanoparticles (25 nm in diameter) were integrated into the gels. The release of vitamin B_{12} loaded in these gels was studied in the presence of an AMF (2.98 kA/m @ 297 Hz). It was shown that when the AMF was applied, heat generation of the magnetic nanoparticles increased the temperature of the NIPAAm network above the LCST, leading to gel collapse and excretion of the water out of the polymer matrix. This process increased the release rate of the B_{12} from the polymeric matrix.[46] In another study done by Hoare et al.[47], thermo-responsive NIPAAm-based nanogels were incorporated in ethyl cellulose-based membrane made containing iron oxide nanoparticles. As in the previous study, this gel formulation was used due to its ability to change its volume at different temperatures When an alternating

magnetic field was applied to these nanogels, the iron oxide nanoparticles contained in the membrane heated up and rose beyond physiological temperatures to 50°C. This heating caused a ~400 nm decrease in the diameter of the nanogels which then led to an outward flux of sodium fluorescein from the drug reservoir (Figure 2).

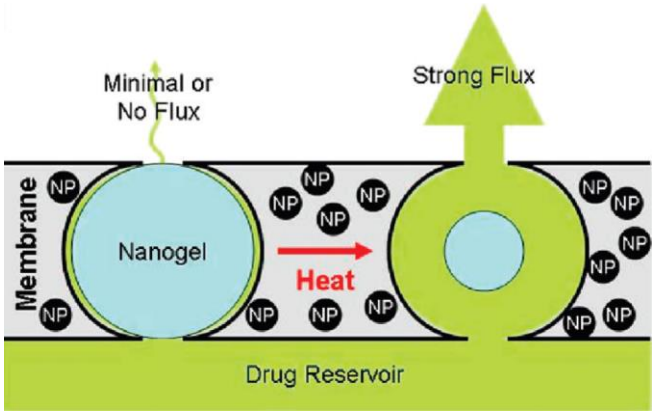

Figure 0.2. Schematic of Magnetically responsive membrane triggered for drug release. Figure copied from Hoare et. al.[47]

Elsewhere, Lu et al.[48] incorporated the ferromagnetic gold coated cobalt nanoparticles inside 5-μm diameter microcapsules made from poly(sodium styrene sulfate)/poly(allylamine hydrochloride). When an AMF was applied, the embedded Co@Au nanoparticles vibrated and disturbed the structure of the microcapsule wall, leading to increases in the permeability of the microcapsule wall. This, in turn, lead to enhanced diffusion of FITC-labeled dextran across the capsule wall (Figure 3).

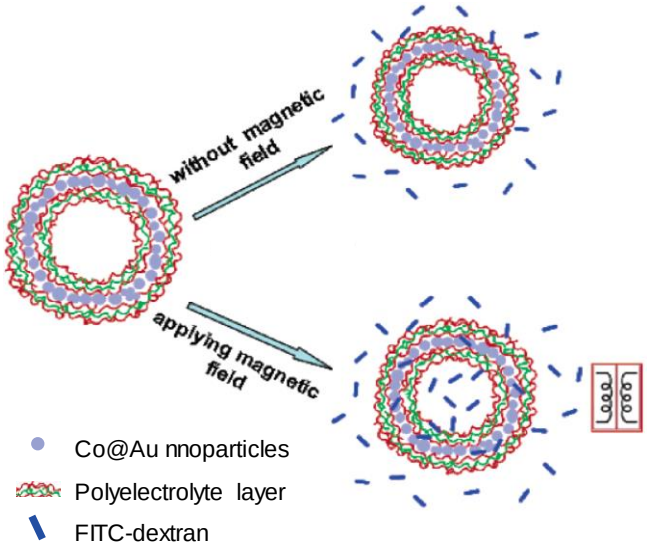

Figure 0.3. Illustration of effect of magnetic field on drug diffusion across microstructures. Figure adapted from Lu et al.,[48]

2.2.2 Physical changes in response to magnetic fields

Magnetic fields can be used to generate forces on magnetic particles and these forces can be used to directly impact physical structures in hydrogel that impact payload retention and release characteristics. For example, magnetic particles can be entrapped within a hydrogel's polymer matrix (Figure 4, left). In the presence of a DC magnetic gradient (e.g., from a hand-held magnet), forces are exerted on the entrapped magnetic particles. This force moves the particles towards the magnet and hydrogel matrix deforms due to this particle movement (Figure 4, right). This deformation results in decrease in gel volume and convective purging of water and loaded drugs from the gel system (Figure 4, right, red dots leaving matrix). For instance, Zhao et al.[49] demonstrated that while some ferrogel deformation could be achieved by simply incorporating iron oxide particles into an alginate hydrogel matrix, generation of a highly macroporous hydrogel

structure (i.e., through a cryogelation approach) yielded much softer and more magnetically compressible ferrogels that were capable of efficiently delivering biological payloads (i.e., chemotherapeutics, proteins, DNAs, and even cells) when subjected to simple hand-held magnets. Zhao et al.[49] went on to demonstrate efficient delivery of cellular payloads in vivo using these same macroporous ferrogels. Subsequent improvements upon these macroporous ferrogels include a biphasic design which enables efficient deformations and payload deliveries using decreased concentrations of iron oxide[35] Additionally, these biphasic ferrogels exhibited increased porosity (for better cellular infiltration) and decreased toxicity (due to lower iron oxide concentrations) for tissue engineering and other in vivo applications. In fact, when implanted in vivo, periodic magnetic deformation of these biphasic gels where shown to reduce inflammation and enhance muscle regeneration.[50]

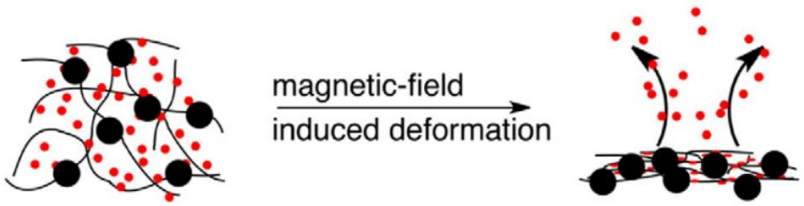

Figure 0.4. Schematic of hydrogel deformation triggered with DC graded magnetic field. Figure adapted from Brundo et al.[44]

Magnetically actuated movement, aggregation, and/or orientation of iron oxide particles can also be used as a means to regulate drug release. For example, magnetically actuated aggregation of magnetic particles can be used to decrease drug delivery rates. A fundamental example of this was demonstrated by Guowei et al.,[51] in which a porous membrane was introduced that seals a depot of magnetic nanospheres containing drug. A

magnetic field was used to aggregate the magnetic particles in a manner that prevented diffusion of the drug through the membrane. In a separate study by Liu et al.,[52] a poly(vinyl alcohol) hydrogel was fabricated with 150-500 nm Fe_3O_4 nanoparticles incorporated into the gel. This ferrogel was used as a membrane that sealed a drug depot. The application of the direct current (DC) magnetic field lead to the aggregation of the Fe_3O_4 nanoparticles in the ferrogel membrane, thus decreasing the porosity of the ferrogel membrane and leading to decreased diffusion of the drug through membrane. Similar ability to modulate drug release using a magnetic field was observed in another study where gelatin ferrogels were used as a membrane.[53] In another study, superparamagnetic iron oxide nanoparticles were embedded inside the Pluronic F127 micelles with diameter around 13 nm. Indomethacin was loaded in another group of micelles and both groups were mixed together inside an aqueous environment (Figure 5, i). Upon application of a magnetic field, SPIONs orient and approach each other, thus perturbing the micelle structures by squeezing them and forcing out the indomethacin drug (Figure 5, ii).[54]

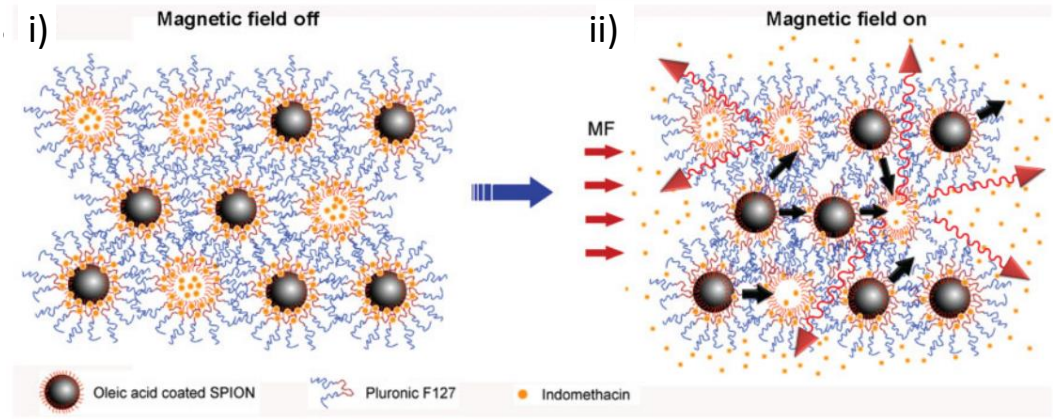

Figure 0.5. Illustrations drug-containing micelles being disrupted in a magnetic field. Figure adapted from Qin et al.[54]

Movement of magnetic particle-laden materials can also be used to modulate drug delivery through the use of micropumps. In a study by Wang et. al.,[55] a microdevice was developed with a drug reservoir placed between two PDMS membranes (Figure 6A, red drug reservoir sandwiched between two blue, flexible PDMS membranes). An iron oxide PDMS composite disk was placed underneath one of the membranes (Figure 6A, yellow composite subjacent to the bottom blue PDMS membrane). This arrangement restricted the diffusion of drug when no magnetic field was applied, as the drug reservoir remained sealed (Figure 6B). However, when a magnetic field was applied, the magnetic-nanoparticle-laden composite would be attracted to the magnet, thus deforming the PDMS membranes, resulting in an arrangement that would facilitate the release of the drug reservoir (Figure 6C). This system was demonstrated successfully both in vitro and in vivo. Researchers have developed similar battery-less magnetically responsive drug delivery devices for delivering docetaxel for treatment of diabetic retinopathy[56] and on-demand insulin administrations[57].

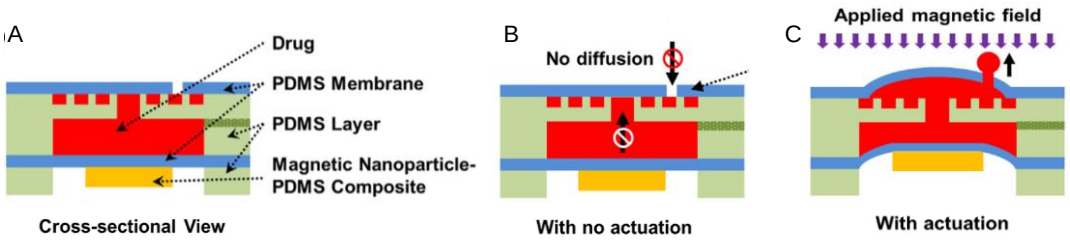

Figure 0.6. The schematic of the intravitreal implantable magnetic micropump. A) Cross section view of the micropump. B) The diffusion of the drug is prevented when there is no magnetic field. C) In the presence of magnetic field, drug releases upward. Figure adapted from Wang et. al[55]

2.3 Tunable parameters affecting drug release

There are several material parameters that impact the retention and magnetically stimulated release of payloads from these biomaterial systems such as ferrogel pore size, magnetic particle concentration and size. As with other hydrogel-based materials, matrix porosity is a critical parameter influencing release characteristics. Generally, a more open more structure results in higher levels of release both unstimulated diffusive release and magnetically stimulated release. However, in many applications, it is desirable to achieve low-levels of unstimulated release and much greater levels of release upon magnetic stimulation. Thus, hydrogel porosity must be tuned to achieved desirably low levels of unstimulated release and desirably high levels of stimulated release. Hydrogel nanoporosity (i.e., the mesh structure of the polymeric matrix) can be tuned by altering polymer and crosslinker concentration.[31–33] Hydrogel macroporosity (i.e., large, often interconnected disruptions in the pores macrostructure) can drastically increase surface area of the gel as well as magnetic compressibility.[35,49]It was shown by Zhao et al.[49]that a

freeze-drying method could be used to generate macroporous ferrogels and that the macropores of the ferrogel could be controlled by the temperature at which the gel was frozen.

Regarding porosity, the incorporation of iron oxide particles into the hydrogel matrix required to endow the hydrogel with magnetic responsiveness has been shown to decrease the porosity of the ferrogels. For both ferrogels that rely on magnetic heating/agitation vs. deformation/aggregation/alignment, this change in porosity certainly impacts release characteristics. Specifically, for magnetically deformable hydrogels, higher concentrations of iron oxide reduces hydrogel porosity, thus reducing magnetic deformability, thus reducing the amount of drug released when the gel is magnetically deformed.[35] However, despite this, increased concentrations of iron oxide may provide more magnetic force generation on the ferrogel, thus enhancing magnetic deformability. Thus, iron oxide concentration is associated with two competing parameters: (i) the ability to exert magnetic force for deforming structures and (ii) the inability to deform structures due to changes in porosity and/or material stiffness. For drug deliveries that rely on magnetic deformation, Cezar et al.[35] demonstrated that optimal concentrations of magnetic particles exist for maximum deformation and drug delivery, with too low of concentrations not generating sufficient force and too high of concentrations resulting in gels that are too stiff. However, Cezar et al. went on to show that these competing parameters could be decoupled by partitioning a hydrogel into two regions: (i) a magnetic-particle-free region that can be designed to be as porous and deformable as possible and (ii) a magnetic-particle-laden region that can be densely packed with particles to generate maximum magnetic force. For delivery strategies involving

magnetic heating/agitation, while magnetic particle concentration likely impacts stimulated and unstimulated diffusion out of the hydrogel[58], studies have mostly shown that increasing magnetic particle concentration increases the degree of heating/agitation, and thus enhances stimulated drug release.[37,38,59]Magnetic particle concentration also impacts the nature by which magnetic fields penetrate and/or are absorbed within the hydrogel structure. In a study conducted by Liu et al.[60] on controlled permeation of drug from ferrogels, sensitivity of PVA-based ferrogels to magnetic fields were studied in terms of permeability coefficient (P) and partition coefficient (H). Results showed that for optimum magnetization there is a critical parameter of free volume per nanoparticle that needs to be met. For their particular gel system, they found 17-34% iron oxide in PVA ferrogels was necessary for optimal magnetic sensitivity.

For both magnetic heating/agitation- and magnetic deformation-based delivery strategies, magnetic particle size also impacts release characteristics. For magnetic heating, the use of particles smaller than 20 nm reduces eddy currents which in turn restricts the heating of the particles.[23] Therefore, traditionally, SPIONs with diameters between 5-28 nm are used as they heat most efficiently when exposed to AMFs in the radio-frequency range (i.e., 100s of kHz), which are simple and relatively inexpensive to produce.[61] For magnetic deformation-based drug delivery strategies, magnetic particle size also plays a key role in determining delivery characteristics. For example, it was shown that when subjected to the same graded DC magnetic field, ferrogels made with smaller iron oxide particles (less than 50 nm particle size) had significantly lower deformation and drug delivery capabilities compared to ferrogels made with larger iron oxide particles (less than 5 μm in size).[35] Thus, if heating/agitation is desired,

nanoparticle-sized SPIONs are desirable whereas if force/deformation is desired, larger (or aggregated) magnetic particles are desired.

Beyond material parameters, the parameters associated with the applied magnetic field itself play a key role in influencing magnetically stimulated release. Specifically, the amplitude, gradient, frequency, proximity, and directionality of the magnetic field can impact release profiles from ferrogels. Higher amplitudes can generate more magnetic heating/agitation and/or more force generation[38,62], though when using larger, ferromagnetic particles the gradient of the magnetic field is more critical than the amplitude per se. Certainly, proximity of the magnetic source impacts both the amplitude and relative gradient of the magnetic signal, so placement of the ferrogel relative to the magnetic source is a critical consideration.

Regarding frequency, its impact on release can be quite complex. At relatively low frequencies, graded magnetic fields can efficiently exert forces on ferromagnetic particles, thus regulating retention and release characteristics in a number of manners (see Section 2.2).[2,49–57,63] Kennedy et al.[63] demonstrated that even at these relatively low frequencies (1 – 550 Hz), the frequency of magnetic stimulation could be used to regulate the rate of drug release from magnetically deformable ferrogels. Specifically, it was demonstrated that molecules did not efficiently release from ferrogels at too low or high of frequencies, but rather, optimally released at some middle frequency (depending on the how the molecule interacted with the hydrogel matrix). This was explained in terms of (i) low frequencies infrequency purging molecules from the gel structure but (ii) high frequencies not efficiently deforming the gel structure due to exceeding the mechanical resonance of the gel. Thus, a given molecule will exhibit a release rate vs. frequency

signature and that different molecules exhibit different release rate vs. frequency signatures. At higher frequencies (< 100 kHz), SPIONs can efficiently adsorb energy from AMFs, resulting in a number of different means to thermally or agitatedly engender release.[2,37–43,47,48,64] However, there is a strong relationship between the frequency of magnetic stimulation, the size and type of the SPION, and the efficiency of AMF absorption.[40,65,66] For example, for a Fe_3O_4 SPION of a given diameter, its heating is a function of AMF frequency, being optimally resonant at a specified frequency. This heating vs. frequency signature is different for different sizes and types of SPIONs, but generally, larger SPIONs are more efficiently heated at AMFs with longer wavelengths (i.e., lower frequencies) and smaller SPIONs are more efficiently heated at AMFs with shorter wavelengths (i.e., higher frequencies).

Finally, the orientation or directionality of the applied magnetic field can impact release characteristics. For example, hand held magnets can align or move magnetic particles in specified directions based on the field lines emanating from the magnet (which is, in turn, based on the way the direction that the magnetic is oriented/held). This orientation/alignment can lead to aggregation of the particles or compression of the gel matrix in specified directions. This can greatly impact release. For instance, when using the system described in Figure 6,[55] orientation of the magnet such that the magnetic PDMS disk (yellow on schematic) is pulled downward would result in tightening of the seal, restricting drug release. Only when pulled upwards would this system provide release. Likewise, for a biphasic ferrogel,[35] orientation of the magnet gradient must result in pulling the iron-oxide-laden region of the gel against the soft, deformable region to

appreciably trigger drug release. If the magnetic gradient is aligned otherwise, the iron-oxide-laden region will not deform the deformable region, thus limiting drug delivery.

2.4 Perspectives on generating temporally complex drug delivery profiles using magnetically responsive hydrogels

2.4.1 Introduction

While the section above outlines the many number of parameters that can influence magnetically triggered release, this parametric abundance provides a wealth of strategies for customizing release properties and uncovers the potentiality of generating more complex delivery profiles using magnetic fields. The ability to generate more complex delivery profiles (e.g., temporally dynamic deliveries that change vs. time and delivery profiles that involve more than one drug such as sequential deliveries) is pervasively required in modern medicine. Illnesses and injuries are often associated with the interruption or distortion of natural sequences of biological events. Thus, therapeutically regulating these sequential biological processes requires sequentially delivering multiple bioactive therapeutics with the proper dosing, timing, and sequence.[29,67–70] Beyond sequential deliveries for therapeutic control over sequential biological processes, the temporal profile of single drug deliveries can be critical for optimizing therapeutic outcome. For example, chronotherapies involve pulsing the delivery of anticancer drugs to increase drug concentration when the tumor is metabolically active and to decrease it when not metabolically active.[29,67,71,72] These pulsatile delivery profiles can also help prevent the tumor from developing an adaptive

resistance to the anticancer drugs.[73,74] Thus, strategies must be developed to generate temporally complex delivery profiles (i.e., pulsed deliveries) and multi-drug, sequential delivery profiles. This section will explore existing strategies for obtaining these types of deliveries and propose potential strategies for obtaining these deliveries moving forward.

2.4.2 Existing strategies

A key advantage to using magnetically responsive hydrogels is that a magnetic field can be applied at times when changes in the delivery profile are desired. Simply put, changes in delivery profile can be regulated in an on-demand manner. Therefore, magnetically responsive hydrogels are theoretically capable of generating temporally complex delivery profiles such as pulsatile deliveries. In a study done by Hu et al,[43] the pulsatile release of vitamin B12 from a gelatin ferrogel was investigated. Ferrogels were exposed to5-minute high-frequency magnetic field (HFMF) pulses with 180 minutes of no magnetic field in between each stimulation. A burst increase in the release rate was observed during each stimulation period (Figure 7). However, a gradual reduction in the release rate was observed over time.

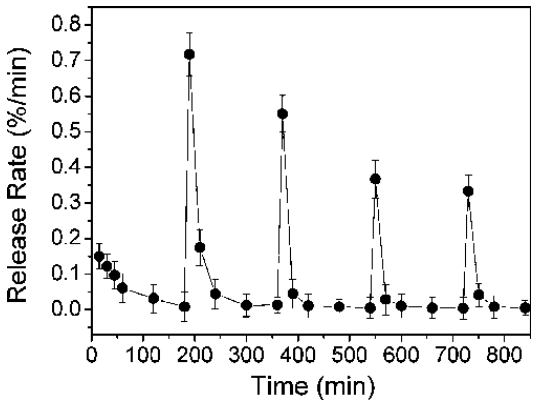

Figure 0.7. Pulsatile drug release rate from gelatin loaded with iron oxide nanoparticles (40 nm in diameter) under 5 minute period of HFMF every 180 minute. Figure taken from Hu et al.[43]

Elsewhere, Satarkar et. al[64] also demonstrated pulsatile delivery of vitamin B12 from (NIPAAm)-based ferrogels. The results showed approximately 6 times increase in the release upon AMF magnetic stimulation for 10 minutes every 20 minutes. Again, however, while a pulsatile delivery profiles was achieved, a gradual decrease in release rate was observed over time upon subsequent pulsing (Figure 8). This may have been due to a short recovery period of 20 minutes where the gel structure doesn't have enough time to recover and stay collapsed, thus, limiting diffusive release over time.

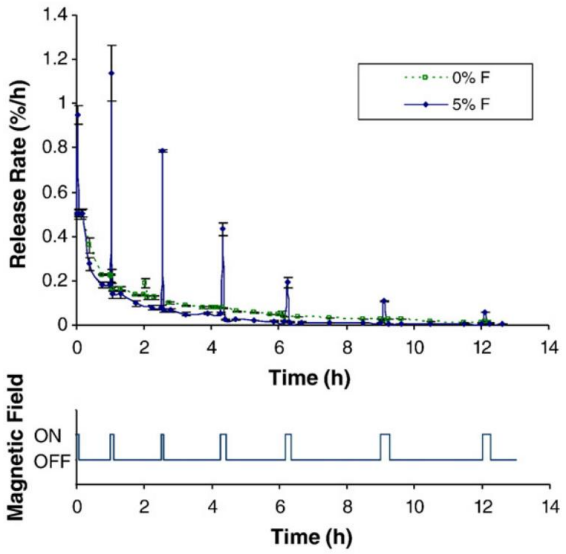

Figure 0.8. Release of Vitamin B_{12} from the nanocomposite upon application of AMF (F). % represents particle loaded by weight in nanocomposite. (N=3±SD). Figure copied from Satarkar et al.[64]

In another study by Emi et al.,[75] magnetically deformable alginate hydrogels were used to generate pulsatile mitoxantrone delivery profiles. However, in this study, pulsatile profiles were produced that were specifically similar to those demonstrated to be highly effective in killing melanoma cells in vitro (one 1-hr pulse of increased mitoxantrone per day for 3 days). This required generating pulsatile delivery profiles over days rather than hours. However, just as in the studies described above,[43,64] over the course of these 3-day experiments, the amount of drug released during magnetic stimulation significantly decreased each day, resulting in pulsatile delivery profiles with diminishing pulse heights. However, to compensate for this, Emi et al. used higher frequencies of magnetic stimulation on subsequent days to maintain delivery rates. This progressive increase in frequency resulted in pulsatile delivery profiles with uniform pulse heights (Figure 9A).

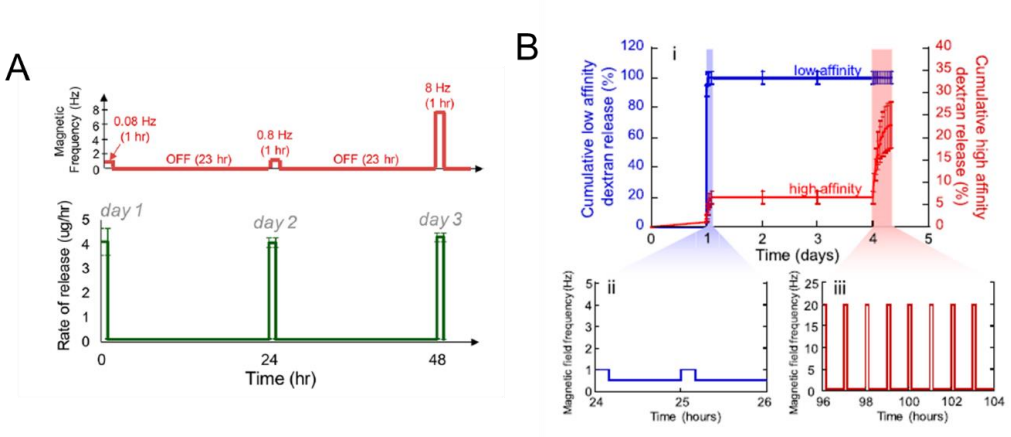

Figure 0.9. A) Demonstration of pulsatile mitoxantrone delivery profiles using magnetic stimulation. Adapted from Emi et al. [75] B) Demonstration of sequential delivery of two model drugs (dextrans: lower affinity in blue, higher affinity in red) vs. time. Adapted from Kennedy et al. [63]

As mentioned above, generation of multi-therapeutic, sequential delivery profiles is also critical in directing biological processes pertinent to injury and disease. While little work has been done in using magnetically responsive hydrogels to achieve these types of complex delivery profiles, Kennedy et al. [63] demonstrated that different molecules with different affinities to a ferrogel's matrix exhibited different release rate vs. frequency (1 – 550 Hz). For instance, this study demonstrated that a dextran with a lower affinity to the alginate ferrogel preferentially released from the ferrogel when stimulated at 1 Hz, whereas a dextran with a higher affinity preferentially released when stimulated at 20 Hz. Thus, a sequential delivery profiles was achieved by first triggering the low affinity dextran to release by stimulating at 1 Hz at earlier time points, followed by triggered release of the high affinity dextran when stimulating at 20 Hz at later time points (Figure 9B). In another study by Tolouei et al.,[76] a dual compartment biomaterial system was introduced that was composed of a gelatin outer compartment surrounding a

ferrogel inner compartment. This study went on to demonstrate that the outer compartment could initially release pro-inflammatory cytokines and the inner ferrogel could delay the delivery of anti-inflammatory cytokines (until magnetically triggered to do so). This 2-copartment biomaterial system was thus capable of generating sequences of pro- and anti-inflammatory cytokine deliveries using the timing of the magnetic stimulation to control the duration between these two deliveries.

2.4.3 Prospective strategies

Despite the importance of developing biomaterials capable of with temporarily complex, multi drug delivery capabilities, there are only a limited number of examples of magnetically responsive systems demonstrating this ability (section 4.2). However, as mentioned above, there are a wealth of tunable parameters that may be employed in future studies that may enable the production of these more complex deliveries. For instance, the location, direction, and/or shape of the applied magnetic field could be used to independently trigger specified release events if a ferrogel is constructed in a compartmentalized manner. If different magnetically compressible compartments are loaded with different drugs (Figure 10A, i: Drugs A (red), B (blue), and C (green)) then an appropriately shaped magnet can be used to only trigger release from a targeted compartment (Figure 10A, ii: only the compartment containing drug B (blue) is compressed). Likewise, the compartments containing drugs A and C can be triggered at on-demand timepoints. This system could coordinate complex delivery profiles involving all three drugs. Similar arrangements could also be used to control not only the selectivity of which drug is being delivery and when, but also some degree of control

over the directionality of drug delivery. For example, if the gel is compartmentalized in a way where different compartments will be deformed when a magnetic is applied from different directions (Figure 10B), then the directionality of drug release can be magnetically regulated. This compartmentalized approach can be applied to membrane reservoir system as described in Section 2 of this chapter as well to achieve control over multiple drug deliveries.

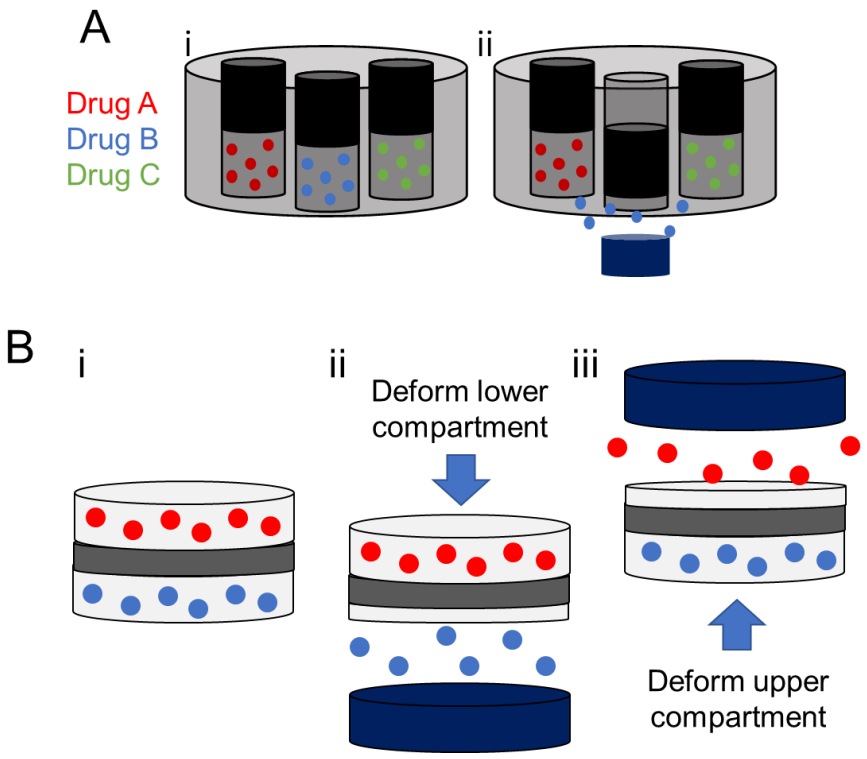

Figure 0.10. A) Illustration of a 3-compartment system for independently triggered deliveries of 3 different drugs. B) Illustration of a compartmentalized hydrogel that can deform, releasing drugs in different directions, depending on from what direction the magnet is applied.

Another way by which magnetic control over multiple deliveries can be achieved is to combine independent mechanisms to independently trigger release. That is, high-

frequency AMFs typically trigger release by heating or physical agitation or disruption and most efficiently influence nano-scale SPIONs. Low-frequency, graded magnetic fields typically trigger release by exerting forces on or aggregating relatively large magnetic particles embedded in the gel. A hydrogel can potentially be constructed by combining these separate elements. One drug (Figure 11, i: red dots) can be loaded into a region of the gel that can deform in response to a graded, low-frequency magnetic field, and a second drug (Figure 11, i: orange lines in blue bubbles) can be loaded into structures that heat, melt, or are disrupted by high-frequency AMFs. Thus, an AMF can be used to independently trigger release of one drug (Figure 11, ii: orange payloads released from blue bubbles) and DC graded magnetic fields can be used to independently trigger release of the other drug (Figure 11, iii: deformation and release of red dots).

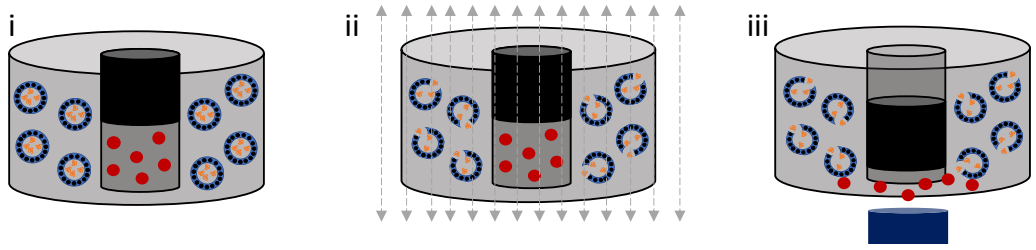

Figure 0.11. Illustration of hydrogel system with the ability to release different drugs when stimulated using different magnetic signals.

Finally, when using SPIONs and AMFs, the efficiency of heating/agitation/disruption is dependent on both the frequency of the AMF and the diameter of the SPION. As mentioned before, generally, smaller SPIONs are more efficiently influenced by higher frequency AMFs whereas larger SPIONs are more efficiently influenced by lower frequency AMFs. This can be exploited in a system where

different structures containing different drugs are preferentially disrupted at different frequencies. Specifically, structures/depots containing drug 1 can be integrated with smaller SPIONs that preferentially respond to higher-frequency AMFs (Figure 12, bubbles decorated with small black dots, containing red drug). Other structures/depots containing a different drug can be integrated with larger SPIONs that preferentially respond to lower-frequency AMFs (Figure 12, bubbles decorated with larger black dots, containing blue drug). Therefore, when stimulated using a relatively low-frequency AMF, the structures decorated with larger SPIONs will preferentially be disrupted, releasing their payloads (Figure 12, middle). When stimulated using a relatively high-frequency AMF, structures decorated with larger SPIONs will preferentially release their payloads (Figure 12, left).

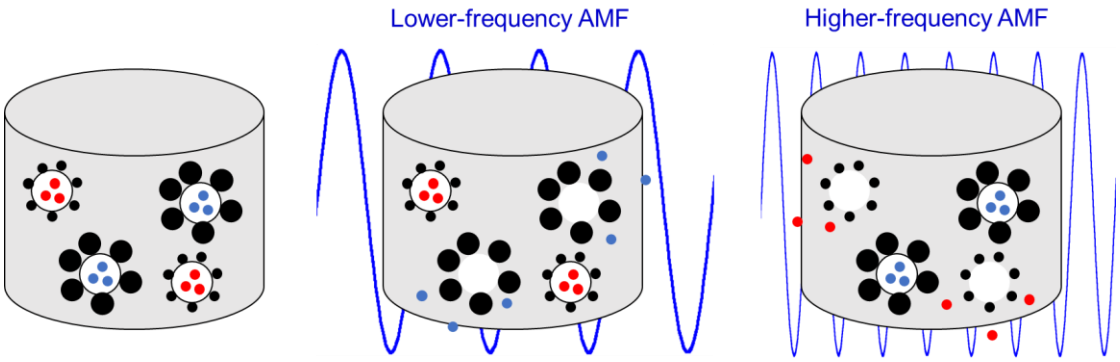

Figure 0.12. Illustration of system containing drug depots that differentially respond to AMFs of different frequencies. This enables frequency-dependent control over what drug is being delivered when.

2.5 References

1. Magnani M. Drug delivery and targeting system. *Emerg Ther Targets*. 1998;2(1):145-146. doi:10.1517/14728222.2.1.145

2. Brudno Y, Mooney DJ. On-demand drug delivery from local depots. *J Control Release*. 2015;219:8-17. doi:10.1016/j.jconrel.2015.09.011

3. Jeong B, Gutowska A. Lessons from nature: Stimuli-responsive polymers and their biomedical applications. *Trends Biotechnol*. 2002;20(7):305-311. doi:10.1016/S0167-7799(02)01962-5

4. Ferreira NN, Ferreira LMB, Cardoso VMO, Boni FI, Souza ALR, Gremião MPD. Recent advances in smart hydrogels for biomedical applications: From self-assembly to functional approaches. *Eur Polym J*. 2018;99(November 2017):117-133. doi:10.1016/j.eurpolymj.2017.12.004

5. Gupta P, Vermani K, Garg S. Hydrogels: From controlled release to pH-responsive drug delivery. *Drug Discov Today*. 2002;7(10):569-579. doi:10.1016/S1359-6446(02)02255-9

6. Balamuralidhara V, Pramodkumar TM, srujana N, et al. pH sensitive drug delivery systems: A review. *Am J Drug Discov Dev*. 2011;1(1):28-48. doi:10.39.23/ajdd.2011.24.48

7. Bromberg LE, Ron ES. Temperature-responsive gels and thermogelling polymer matrices for protein and peptide delivery. *Adv Drug Deliv Rev*. 1998;31(3):197-221. doi:10.1016/S0169-409X(97)00121-X

8. Xu FJ, Kang ET, Neoh KG. pH- and temperature-responsive hydrogels from crosslinked triblock copolymers prepared via consecutive atom transfer radical polymerizations. *Biomaterials*. 2006;27(14):2787-2797. doi:10.1016/j.biomaterials.2006.01.003

9. Singh NK, Lee DS. In situ gelling pH- and temperature-sensitive biodegradable block copolymer hydrogels for drug delivery. *J Control Release*. 2014;193:214-227. doi:10.1016/j.jconrel.2014.04.056

10. Alvarez-Lorenzo C, Bromberg L, Concheiro A. Light-sensitive intelligent drug delivery systems. *Photochem Photobiol*. 2009;85(4):848-860. doi:10.1111/j.1751-1097.2008.00530.x

11. Kennedy S, Bencherif S, Norton D, Weinstock L, Mehta M, Mooney D. Rapid and Extensive Collapse from Electrically Responsive Macroporous Hydrogels. *Adv Healthc Mater*. 2014;3(4):500-507. doi:10.1002/adhm.201300260

12. Huebsch N, Kearney CJ, Zhao X, et al. Ultrasound-triggered disruption and self-healing of reversibly cross-linked hydrogels for drug delivery and enhanced chemotherapy. *Proc Natl Acad Sci U S A*. 2014;111(27):9762-9767. doi:10.1073/pnas.1405469111

13. Priya James H, John R, Alex A, Anoop KR. Smart polymers for the controlled delivery of drugs – a concise overview. *Acta Pharm Sin B*. 2014;4(2):120-127. doi:10.1016/j.apsb.2014.02.005

14. Oh JK, Park JM. Iron oxide-based superparamagnetic polymeric nanomaterials: Design, preparation, and biomedical application. *Prog Polym Sci*. 2011;36(1):168-

189. doi:10.1016/j.progpolymsci.2010.08.005

15. Barbucci R, Giani G, Fedi S, Bottari S, Casolaro M. Biohydrogels with magnetic nanoparticles as crosslinker: Characteristics and potential use for controlled antitumor drug-delivery. *Acta Biomater*. 2012;8(12):4244-4252. doi:10.1016/j.actbio.2012.09.006

16. Medeiros SF, Santos AM, Fessi H, Elaissari A. Stimuli-responsive magnetic particles for biomedical applications. *Int J Pharm*. 2011;403(1-2):139-161. doi:10.1016/j.ijpharm.2010.10.011

17. Laurent S, Forge D, Port M, et al. Magnetic Iron Oxide Nanoparticles: Synthesis, Stabilization, Vectorization, Physicochemical Characterizations, and Biological Applications (vol 108, pg 2064, 2008). *Chem Rev*. 2008;108(6):2064-2110. doi:Doi 10.1021/Cr900197g

18. Estelrich J, Escribano E, Queralt J, Busquets MA. Iron oxide nanoparticles for magnetically-guided and magnetically-responsive drug delivery. *Int J Mol Sci*. 2015;16(4):8070-8101. doi:10.3390/ijms16048070

19. Preiss MR, Bothun GD. Stimuli-responsive liposome-nanoparticle assemblies. *Expert Opin Drug Deliv*. 2011;8(8):1025-1040. doi:10.1517/17425247.2011.584868

20. Yilmaz A, Rösch S, Yildiz H, Klumpp S, Sechtem U. First multiparametric cardiovascular magnetic resonance study using ultrasmall superparamagnetic iron oxide nanoparticles in a patient with acute myocardial infarction: New vistas for the clinical application of ultrasmall superparamagnetic iron oxide. *Circulation*.

2012;126(15):1932-1934. doi:10.1161/CIRCULATIONAHA.112.108167

21. Iv M, Telischak N, Feng D, Holdsworth SJ, Yeom KW, Daldrup-Link HE. Clinical applications of iron oxide nanoparticles for magnetic resonance imaging of brain tumors. *Nanomedicine*. 2015;10(6):993-1018.

22. Wang Y-XJ. Superparamagnetic iron oxide based MRI contrast agents: Current status of clinical application. *Quant Imaging Med Surg*. 2011;1(Dcc):35-44. doi:10.3978/j.issn.2223-4292.2011.08.03

23. Chalovich JM, Eisenberg E. Cancer Theranostics: The Rise of Targeted Magnetic Nanoparticles. *Magn Reson Imaging*. 2013;31(3):477-479. doi:10.1016/j.immuni.2010.12.017.Two-stage

24. Ang KL, Venkatraman S, Ramanujan R V. Magnetic PNIPA hydrogels for hyperthermia applications in cancer therapy. *Mater Sci Eng C*. 2007;27(3):347-351. doi:10.1016/j.msec.2006.05.027

25. Shinkai M. Functional magnetic particles for medical application. *J Biosci Bioeng*. 2002;94(6):606-613. doi:10.1016/S1389-1723(02)80202-X

26. Purushotham S, Ramanujan R V. Thermoresponsive magnetic composite nanomaterials for multimodal cancer therapy. *Acta Biomater*. 2010;6(2):502-510. doi:10.1016/j.actbio.2009.07.004

27. Sun C, Lee JSH, Zhang M. Magnetic nanoparticles in MR imaging and drug delivery. *Adv Drug Deliv Rev*. 2008;60(11):1252-1265. doi:10.1016/j.addr.2008.03.018

28. Knipe JM, Peppas NA. Multi-responsive hydrogels for drug delivery and tissue engineering applications. *Regen Biomater*. 2014;1(1):57-65. doi:10.1093/rb/rbu006

29. Peppas NA, Leobandung W. Stimuli-sensitive hydrogels: Ideal carriers for chronobiology and chronotherapy. *J Biomater Sci Polym Ed*. 2004;15(2):125-144. doi:10.1163/156856204322793539

30. Levental I, Georges PC, Janmey PA. Soft biological materials and their impact on cell function. *Soft Matter*. 2007;3(3):299-306. doi:10.1039/B610522J

31. Hoffman AS. Hydrogels for biomedical applications. *Adv Drug Deliv Rev*. 2012;64(SUPPL.):18-23. doi:10.1016/j.addr.2012.09.010

32. Lee KY, Mooney DJ. Hydrogels for tissue engineering. *Chem Rev*. 2001;101(7):1869-1879. doi:10.1021/cr000108x

33. Drury JL, Mooney DJ. Hydrogels for tissue engineering: Scaffold design variables and applications. *Biomaterials*. 2003;24(24):4337-4351. doi:10.1016/S0142-9612(03)00340-5

34. Auernhammer GK, Collin D, Martinoty P. Viscoelasticity of suspensions of magnetic particles in a polymer: Effect of confinement and external field. *J Chem Phys*. 2006;124(20). doi:10.1063/1.2199847

35. Cezar C a, Kennedy SM, Mehta M, et al. Biphasic Ferrogels for Triggered Drug and Cell Delivery. *Adv Healthc Mater*. 2014:1-8. doi:10.1002/adhm.201400095

36. Gonzalez JS, Nicolás P, Ferreira ML, Avena M, Lassalle VL, Alvarez VA.

Fabrication of ferrogels using different magnetic nanoparticles and their performance on protein adsorption. *Polym Int*. 2014;63(2):258-265. doi:10.1002/pi.4498

37. Crippa F, Moore TL, Mortato M, et al. Dynamic and biocompatible thermo-responsive magnetic hydrogels that respond to an alternating magnetic field. *J Magn Magn Mater*. 2017;427(October 2016):212-219. doi:10.1016/j.jmmm.2016.11.023

38. Brazel CS. Magnetothermally-responsive nanomaterials: Combining magnetic nanostructures and thermally-sensitive polymers for triggered drug release. *Pharm Res*. 2009;26(3):644-656. doi:10.1007/s11095-008-9773-2

39. Liu TY, Hu SH, Liu DM, Chen SY, Chen IW. Biomedical nanoparticle carriers with combined thermal and magnetic responses. *Nano Today*. 2009;4(1):52-65. doi:10.1016/j.nantod.2008.10.011

40. Rosensweig REE. Heating magnetic fluid with alternating magnetic field. *J Magn Magn Mater*. 2002;252(0):370-374. doi:10.1016/S0304-8853(02)00706-0

41. Hergt R, Dutz S, Müller R, Zeisberger M. Magnetic particle hyperthermia: Nanoparticle magnetism and materials development for cancer therapy. *J Phys Condens Matter*. 2006;18(38):2919-2934. doi:10.1088/0953-8984/18/38/S26

42. Ward MA, Georgiou TK. Thermoresponsive polymers for biomedical applications. *Polymers (Basel)*. 2011;3(3):1215-1242. doi:10.3390/polym3031215

43. Hu SH, Liu TY, Liu DM, Chen SY. Controlled pulsatile drug release from a

ferrogel by a high-frequency magnetic field. *Macromolecules*. 2007;40(19):6786-6788. doi:10.1021/ma0707584

44. Brudno Y, Mooney DJ. On-demand drug delivery from local depots. *J Control Release*. 2015;219:8-17. doi:10.1016/j.jconrel.2015.09.011

45. Schild HG. Poly(N-isopropylacrylamide): experiment, theory and application. *Prog Polym Sci*. 1992;17(2):163-249. doi:10.1016/0079-6700(92)90023-R

46. Satarkar NS, Hilt JZ. Magnetic hydrogel nanocomposites for remote controlled pulsatile drug release. *J Control Release*. 2008;130(3):246-251. doi:10.1016/j.jconrel.2008.06.008

47. Hoare T, Santamaria J, Goya GF, et al. A magnetically-triggered composite membrane for on-demand drug delivery. *Nanoletters*. 2011;9(10):3651-3657. doi:10.1021/nl9018935.A

48. Lu Z, Prouty MD, Quo Z, Golub VO, Kumar CSSR, Lvov YM. Magnetic switch of permeability for polyelectrolyte microcapsules embedded with Co@Aunanoparticles. *Langmuir*. 2005;21(5):2042-2050. doi:10.1021/la047629q

49. Zhao X, Kim J, Cezar C a, et al. Active scaffolds for on-demand drug and cell delivery. *Proc Natl Acad Sci U S A*. 2011;108(1):67-72. doi:10.1073/pnas.1007862108

50. Cezar CA, Roche ET, Vandenburgh HH, Duda GN, Walsh CJ, Mooney DJ. Biologic-free mechanically induced muscle regeneration. *Proc Natl Acad Sci*. 2016;113(6):1534-1539. doi:10.1073/pnas.1517517113

51. Guowei D, Adriane K, Chen X, Jie C, Yinfeng L. PVP magnetic nanospheres: Biocompatibility, in vitro and in vivo bleomycin release. *Int J Pharm*. 2007;328(1 SPEC. ISS.):78-85. doi:10.1016/j.ijpharm.2006.07.042

52. Liu T-Y, Hu S, Liu T-Y, Liu D, Chen S. Magnetic-Sensitive Behavior of Intelligent Ferrogels for Controlled Release of Drug. *Langmuir*. 2006;22(14):5974-5978. doi:10.1021/la060371e

53. Hu SH, Liu TY, Liu DM, Chen SY. Nano-ferrosponges for controlled drug release. *J Control Release*. 2007;121(3):181-189. doi:10.1016/j.jconrel.2007.06.002

54. Qin J, Asempah I, Laurent S, Fornara A, Muller RN, Muhammed M. Injectable superparamagnetic ferrogels for controlled release of hydrophobic drugs. *Adv Mater*. 2009;21(13):1354-1357. doi:10.1002/adma.200800764

55. Wang C, Seo SJ, Kim JS, et al. Intravitreal implantable magnetic micropump for on-demand VEGFR-targeted drug delivery. *J Control Release*. 2018;283(May):105-112. doi:10.1016/j.jconrel.2018.05.030

56. Pirmoradi FN, Jackson JK, Burt HM, Chiao M. On-demand controlled release of docetaxel from a battery-less MEMS drug delivery device. *Lab Chip*. 2011;11(16):2744-2752. doi:10.1039/C1LC20134D

57. Lee SH, Lee Y Bin, Kim BH, et al. Implantable batteryless device for on-demand and pulsatile insulin administration. *Nat Commun*. 2017;8(May 2016):1-10. doi:10.1038/ncomms15032

58. Satarkar NS, Zach Hilt J. Hydrogel nanocomposites as remote-controlled biomaterials. *Acta Biomater*. 2008;4(1):11-16. doi:10.1016/j.actbio.2007.07.009

59. Papaphilippou P, Christodoulou M, Marinica OM, et al. Multiresponsive polymer conetworks capable of responding to changes in pH, temperature, and magnetic field: Synthesis, characterization, and evaluation of their ability for controlled uptake and release of solutes. *ACS Appl Mater Interfaces*. 2012;4(4):2139-2147. doi:10.1021/am300144w

60. Liu TY, Hu SH, Liu KH, Liu DM, Chen SY. Study on controlled drug permeation of magnetic-sensitive ferrogels: Effect of Fe3O4 and PVA. *J Control Release*. 2008;126(3):228-236. doi:10.1016/j.jconrel.2007.12.006

61. Mehdaoui B, Meffre A, Carrey J, et al. Optimal size of nanoparticles for magnetic hyperthermia: A combined theoretical and experimental study. *Adv Funct Mater*. 2011;21(23):4573-4581. doi:10.1002/adfm.201101243

62. Jalili NA, Muscarello M, Gaharwar AK. Nanoengineered thermoresponsive magnetic hydrogels for biomedical applications. *Bioeng Transl Med*. 2016;1(3):297-305. doi:10.1002/btm2.10034

63. Kennedy S, Roco C, Déléris A, et al. Improved magnetic regulation of delivery profiles from ferrogels. *Biomaterials*. 2018;161:179-189. doi:10.1016/j.biomaterials.2018.01.049

64. Satarkar NS, Hilt JZ. Magnetic hydrogel nanocomposites for remote controlled pulsatile drug release. *J Control Release*. 2008;130(3):246-251. doi:10.1016/j.jconrel.2008.06.008

65. Sato I, Umemura M, Mitsudo K, et al. Simultaneous hyperthermia-chemotherapy with controlled drug delivery using single-drug nanoparticles. *Sci Rep*. 2016;6(April):1-12. doi:10.1038/srep24629

66. Mertz D, Sandre O, Bégin-Colin S. Drug releasing nanoplatforms activated by alternating magnetic fields. *Biochim Biophys Acta - Gen Subj*. 2017;1861(6):1617-1641. doi:10.1016/j.bbagen.2017.02.025

67. Mormont MC, Levi F. Cancer chronotherapy: Principles, applications, and perspectives. *Cancer*. 2003;97(1):155-169. doi:10.1002/cncr.11040

68. Richardson TP, Peters MC, Ennett AB, Mooney DJ. Polymeric system for dual growth factor delivery. *Nat Biotech*. 2001;19(11):1029-1034. http://dx.doi.org/10.1038/nbt1101-1029.

69. Brudno Y, Ennett-Shepard AB, Chen RR, Aizenberg M, Mooney DJ. Enhancing microvascular formation and vessel maturation through temporal control over multiple pro-angiogenic and pro-maturation factors. *Biomaterials*. 2013;34(36):9201-9209. doi:10.1016/j.biomaterials.2013.08.007

70. Mehta M, Schmidt-bleek K, Duda GN, Mooney DJ. Biomaterial delivery of morphogens to mimic the natural healing cascade in bone ☆. *Adv Drug Deliv Rev*. 2012;64(12):1257-1276. doi:10.1016/j.addr.2012.05.006

71. Mormont MC, Lévi F. Circadian-system alterations during cancer processes: A review. *Int J Cancer*. 1997;70(2):241-247. doi:10.1002/(SICI)1097-0215(19970117)70:2<241::AID-IJC16>3.0.CO;2-L

72. Ratner BD, Hoffman AS, Schoen FJ, Lemons JE. Application of Biomaterials: Implants and Inserts. In Biomaterials Science: An Introduction to Materials in Medicine. In: Ratner BD, Hoffman AS, Schoen FJ, Lemons JEBT-BS (Third E, eds. Academic Press. Waltham, MA.; 2013:1062-1068. doi:https://doi.org/10.1016/B978-0-08-087780-8.00153-4

73. Cara S, Tannock IF. Retreatment of patients with the same chemotherapy: Implications for clinical mechanisms of drug resistance. *Ann Oncol*. 2001;12(1):23-27. doi:10.1023/A:1008389706725

74. Goldman A, Majumder B, Dhawan A, et al. Temporally sequenced anticancer drugs overcome adaptive resistance by targeting a vulnerable chemotherapy-induced phenotypic transition. *Nat Commun*. 2015;6:1-13. doi:10.1038/ncomms7139

75. Emi T, Barnes T, Orton E, et al. Pulsatile Chemotherapeutic Delivery Profiles Using Magnetically Responsive Hydrogels. *ACS Biomater Sci Eng*. 2018. doi:10.1021/acsbiomaterials.8b00348

76. Tolouei AE, Dülger N, Ghatee R, Kennedy S. A Magnetically Responsive Biomaterial System for Flexibly Regulating the Duration between Pro- and Anti-Inflammatory Cytokine Deliveries. *Adv Healthc Mater*. 2018;7(12). doi:10.1002/adhm.201800227

Chapter 3

Manuscript (I): A magnetically responsive biomaterial system for flexibly regulating the duration between pro- and anti-inflammatory cytokine deliveries

Published in the *Advanced Healthcare Materials Journal*, April 2018

By Anita E. Tolouei, Nihan Dülger, Rosa Ghatee, Stephen Kennedy*

Department of Chemical Engineering,

University of Rhode Island, Kingston, Rhode Island 02881

* Corresponding author: Stephen Kennedy

Email: smkennedy@uri.edu,

Phone: (401) 874-5295,

Fax: (401) 782-6422

3.1 Abstract

While inflammation can be problematic, it is nonetheless necessary for proper tissue regeneration. However, it remains unclear how the magnitude and duration of the inflammatory response impacts regenerative outcome. This is partially due to the difficulty in temporally regulating macrophage phenotype at wound sites. Here, a magnetically responsive biomaterial system potentially capable of temporally regulating macrophage phenotypes through sequential, on-demand cytokine deliveries is presented. This material system is designed to (i) rapidly recruit proinflammatory macrophages (M1) through initial cytokine deliveries and (ii) subsequently transition macrophages toward anti-inflammatory phenotypes (M2s) through delayed, magnetically triggered cytokine release. Here, the ability of this system to initially deliver proinflammatory cytokines (i.e., monocyte chemoattractant protein-1 and interferon gamma), recruit, and harbor an expanding macrophage population, and delay deliveries of anti-inflammatory cytokines (i.e., IL-4 and IL-10) until the application of magnetic fields from simple hand-held magnets is demonstrated. Critically, the timing and rate of these delayed deliveries can be remotely/magnetically controlled. This biomaterial system can provide a powerful tool in (i) understanding the relationship between inflammation and regenerative outcome, (ii) developing optimized cytokine delivery strategies, and (iii) clinically implementing those optimized delivery strategies with the on-demand versatility needed to alter the course of therapies in real time.

3.2 Introduction

It has been estimated that 1 to 2% of the population in developed countries will experience a chronic wound over their lifespan.[1] Occurrence of chronic wounds are particularly common in growing elderly populations and those who are suffering from diabetes and obesity.[2] While there are several phases in wound healing (i.e., coagulation, inflammation, proliferation, and remodeling),[3–6] chronic wounds are typically the result of prolonged and/or uncontrolled inflammation.[2,7] Despite this, inflammation is an indispensable step in the wound healing process and sets the stage for proper regeneration by staving off infection, clearing the wound site of debris, and recruiting cells to the wound that play critical roles in tissue remodeling and re-vascularization.[3,6,8,9] In fact, studies have shown that suppressing the inflammatory response actually hinders proper wound healing.[4,10] Macrophages play a key role in regulating the inflammatory response and in directing the transition to later stages of the wound healing process.[11–17] We and others believe that regulating the time at which macrophages transition from coordinating an inflammatory response (Figure 1.a, Phase 1 (red)) to coordinating later pro-healing stages of the wound healing process (Phase 2 (blue)) may be key to understanding the role of inflammation in wound healing and in developing improved treatment strategies.[18–20] For example, it is apparent that proper healing requires an inflammatory phase that eventually transitions into anti-inflammatory, pro-healing phases.[21,22] However, it remains unknown how the *duration* of this inflammatory phase (T_{ih}) impacts or can be used to optimize wound healing outcome. Moreover, optimal durations are likely different for different wounds and for different patients. This motivates the need for biomaterials that enable flexible control over the duration of this inflammatory period,

as both an investigative and clinical tool.

Here, we propose a biomaterial system designed to deliver immunomodulatory cytokines in a manner that can potentially regulate the inflammatory period's duration in a flexible and on-demand manner. The inflammation phase can be initiated by establishing a population of pro-inflammatory M1 macrophages through the delivery of proteins that recruit macrophages and polarize them towards M1 phenotypes (Figure 1.b, M0 to M1): for example, Monocyte Chemoattractant Protein-1 (MCP-1),[23,24] and Interferon Gamma (IFN-γ).[25] Transition from inflammatory to healing phases requires establishing a population of anti-inflammatory M2 macrophages (e.g., alternatively activated M2a, Mb, and Mc phenotypes). This can be triggered through the delivery of other proteins at the wound site: for example, Interleukin-4 (IL-4),[26,27] and Interleukin-10 (IL-10),[26,27] (Figure 1.b, M0/M1 to M2).

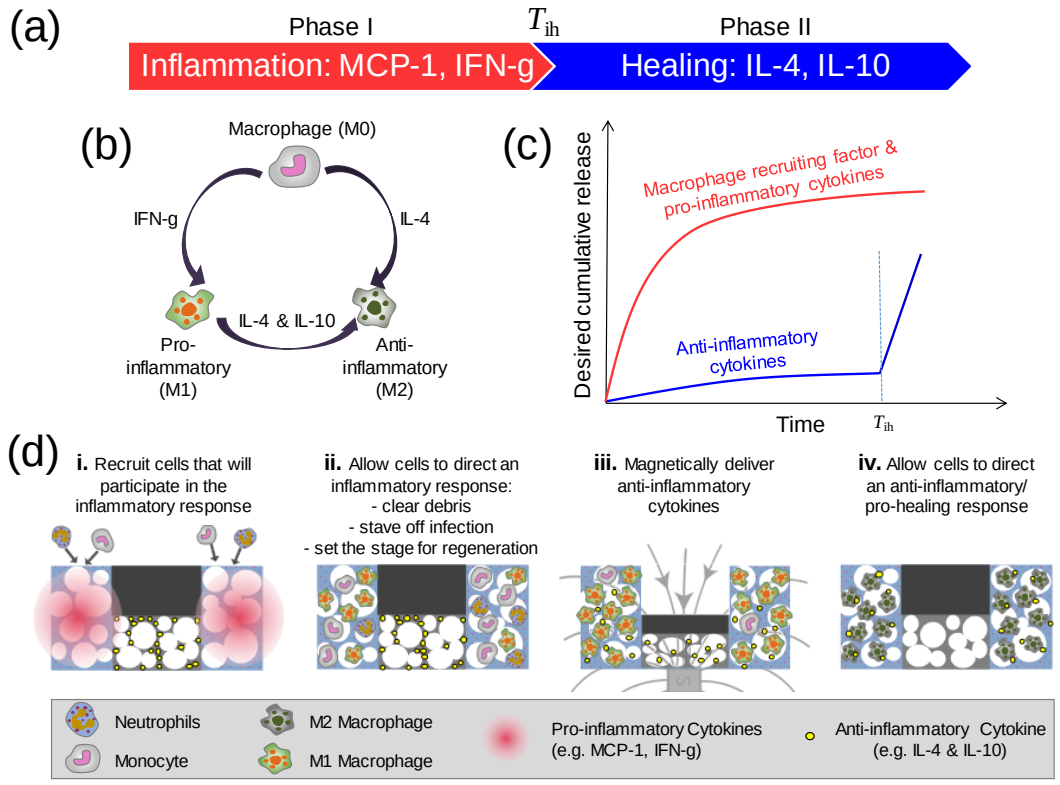

Figure 0.1. Regulating the inflammatory period requires initial delivery of pro-inflammatory cytokines followed by delayed delivery of anti-inflammatory cytokines. (a) Schematic describing the cytokines that regulate the inflammation phase (I, red) and healing phase (II, blue). (b) Schematic describing how M0 macrophages can be polarized into M1 (Pro-inflammatory) and/or M2 (Anti-inflammatory) phenotypes when exposed to different cytokines. (c) Illustration of the desired cumulative release profile: initial release of macrophage recruitment and pro-inflammation cytokines (red), followed by delivery of anti-inflammatory cytokines (blue). (d) Illustration of the proposed biomaterial system (top) with illustration key (bottom).

Thus, it may be possible to regulate the duration of the inflammatory response (T_{ih}) through initial deliveries of pro-inflammatory cytokines, such as MCP-1 and IFN-γ (Figure 1.c, red curve), followed by delayed deliveries of anti-inflammatory cytokines, such as IL-4 and/or IL-10 (Figure 1.c, blue curve). Here, we will describe a two-compartment biomaterial system (Figure 1.d) designed to: (i) initially release pro-inflammatory cytokines from an outer compartment for the recruitment and establishment of pro-inflammatory macrophage phenotypes, (ii) allow for an inflammatory period to

continue until, (iii) a magnetic gradient is applied that deforms the inner compartment, releasing anti-inflammatory cytokines, which would (iv) direct macrophages to take on pro-healing phenotypes. Such a material system could enable control over the inflammatory period's duration simply by applying a magnetic gradient (from simple hand-held magnets or electromagnets) at the time point at which one wishes inflammation to transition into an anti-inflammatory phase.

3.3 Materials and methods

3.3.1 Fabrication and imaging of the biomaterial system

The outer compartment gelatin scaffolds used in these studies were purchased as 2 x 12 x 7 mm GelFoam™ sponge sheets (Pfizer, Groton, CT) and cut into hollow disks (2-mm tall, 8-mm OD, 4-mm ID) using 8-mm and 4-mm biopsy punches. Note that biopsy punches and GelFoam sponges were packaged sterile for cell experiments. Additionally, they were packaged in lyophilized form, allowing them to be sputter-coated (30 seconds in gold) and imaged under Scanning Electron Microscopy (SEM) on a Zeiss SIGMA VP Field Emission-SEM with cryogenic capability and Energy-dispersive X-ray Spectroscopy (EDS) for elemental mapping.

The inner ferrogel compartments were made similarly to those described in Cezar et al.[28] Briefly, alginate was dissolved in MES buffer (100 mM MES and 500 mM NaCl at pH = 6.0) containing HOBT and AAD crosslinker and was cast with iron oxide particles and EDC (100 mg mL^{-1}) between two Sigmacote-treated glass plates that were separated by 2-mm spacers. During casting (~ 1 hour), a magnet was placed against one

glass plate as to pull the iron oxide particles towards one side of the gel, yielding a biphasic structure. Individual biphasic ferrogels were cut into 4 x 2 mm disks using a biopsy punch and then washed in 50 mL deionized water for 3 days (with water being exchanged twice a day) so that they would fully swell and become void of residual reagents. Ferrogels were then frozen at -20 ºC overnight and lyophilized. Lyophilized ferrogels were prepared for imaging by cross sectioning them using a sharp razor, sputter-coating in gold, and imaging as described above for the outer gelatin scaffolds.

3.3.2 Macrophage recruitment studies

In their culture flasks, RAW 264.7 mouse macrophages were rinsed in PBS, resuspended in fresh DMEM, scraped off, collected, and plated at 10,000 cells per well on sterile 12-well plates. Macrophages were submerged in serum-containing DMEM and allowed to grow for 24 hours. A sterile gelatin scaffold (cut into a hollow disk) was then placed on top of the 2D culture in well plates (fully submerged in media) and left to recruit macrophages for 10 days. Macrophage-populated gelatin scaffolds were analyzed by fixing them in 4% PFA for 10 minutes and washed for 5 minutes in PBS, 3 times. Scaffolds were then soaked in a 0.2% Triton X-100/PBS solution for 5 minutes to permeabilize cell membranes, then washed for 5 minutes in fresh PBS, 3 times. Macrophage nuclei were DAPI-stained by soaking scaffolds in a 2 μg/mL solution of DAPI in PBS for 5 minutes and then washing for 5 minutes in fresh PBS, 3 times. Finally, macrophage actin cytoskeletons were stained by soaking scaffolds in a 0.5 μg/mL solution of FITC-phalloidin in PBS for 5 minutes and then washing for 5 minutes in fresh PBS, 3 times.

3D fluorescent image reconstructions were obtained by taking a green/blue

confocal slice every 10 μm from the bottom of the scaffold to a depth of 170 μm within the scaffold using a Nikon TE2000E inverted confocal microscope and its associated NIS-Elements software package. Macrophage cell density counts were taken by inverting the gels in a fresh 12-well plate so that the top of the gels faced down against the plate. Well plates were then loaded into a BioTek Cytation 3 Cell Imaging Multi-Mode Reader which was set to capture a blue-channel image 200 μg into the scaffold (which was 1800 μm away from the side of the scaffold originally near the 2D macrophage culture). BioTek Gen5 software was used to quantify DAPI-nuclei count from these blue-channel images.

3.3.3 Magnetic stimulation of ferrogels

Ferrogels were magnetically stimulated using 0.5” x 0.5” x 0.5” (1.32 x 1.32 x 1.32 cm) cylindrical neodymium magnets (K&J Magnetics, Pipersville, PA) that were integrated into a custom stimulation apparatus that enabled repetitive and prolonged magnetic field exposures. The custom stimulation apparatus consisted of an array of cylindrical neodymium magnets place on the teetering edge of a variable-speed laboratory rocker’s platform (4 magnets on one edge and 4 on the opposite edge, see MovieS2 in supporting information). This arrangement allowed 8 magnets to oscillate up and down (proximally and distally to 8 ferrogel samples) at a rate prescribed by the rocker’s speed. These studies all utilized the maximum rate of 1.4 Hz (i.e., one magnetic compression every 0.71 seconds). Ferrogels were placed in Sigmacote-treated scintillation vials and suspended above our custom stimulation apparatus with aluminum clamps. This arrangement allowed ferrogel samples to be in close proximity to the magnetics when the magnets were raised (though the magnets did not physically touch

the vials) and far enough away from the magnets (~10 cm) when the magnets were lowered, allowing the ferrogels to fully compress and conform back to their original un-compressed thickness between each cycle.

3.3.4 Cytokine time course release studies

Outer compartment gelatin scaffolds were unpacked and punched to shape in a lyophilized state. Thus, to load them with cytokine, concentrated solutions of protein were prepared and added dropwise directly to the dehydrated scaffolds. It was determined beforehand that when adding liquid to these scaffolds in this manner, they could fully absorb no more than 40 μL of solution. Thus, when loading the scaffolds, concentrated solutions were prepared such that the desired amount of protein to be loaded in the scaffold be contained in 40 μL volumes (e.g., 1000 ng MCP-1 loading required preparation of a concentrated solution of 1000 ng MCP-1 in 40 μL of PBS). So, scaffolds were placed in Sigmacote-treated scintillation vials (to limit protein adsorption to the surfaces of the vials) and loaded dropwise with concentrated protein solutions (MCP-1 or IFN-γ, prepared at concentrations as described above). Scintillation vials were then capped and the scaffolds were left overnight at room temperature to fully absorb the protein. Time-course release studies began after overnight protein absorption when scaffolds were submerged in 1 mL PBS with 1% BSA (t = 0). 1 mL samples were collected periodically from the vials and reserved for analysis by freezing in 1.5 mL centrifuge tubes. After sample removal, fresh 1 mL of PBS with 1% BSA was gently added back to the vial until the next sample was taken. After all samples were collected (168 hours), they were thawed and quantified for cytokine content using ELISA.

Release studies from ferrogels followed a similar procedure. As described above, ferrogels were prepared with the final step being lyophilization, thus producing macroporous and dehydrated samples. Dried ferrogels were placed in scintillation vials with the Fe_3O_4-free region facing up. It was determined beforehand that when adding liquid to these ferrogels that they could fully absorb no more than 20 μL of solution. They were therefore loaded using desired weights of protein dissolved in 20 μL of PBS (e.g., 1000 ng IL-4 in 20 μL PBS). Ferrogels were left to absorb the protein overnight in capped vials. Ferrogels were then rinsed in PBS with 1% BSA for 3 days to remove excess unincorporated protein, which reduced unstimulated baseline release. Ferrogels were then periodically sampled as described with the gelatin scaffolds, with sample media being fully removed and replaced with fresh media at each timepoint. Collected samples were quantitatively analyzed for IL-4 or IL-10 release using ELISA.

3.3.5 Statistical analyses

All quantitative data presented in this communication are represented as a mean ± standard deviation with 4 replicates (N = 4). Because only one-to-one statistical comparisons were made in this study (i.e., no multiple comparisons), student t-tests (two-tailed distributions, heteroscedastic) were used to calculate *p*-values with $p < 0.05$ being our benchmark for significance (Microsoft Excel).

3.4 Results and discussion

This two-compartment biomaterial system comprises an outer gelatin scaffold and an inner biphasic ferrogel (Figure 2.a). The outer compartment exhibited an interconnected macroporous structure designed to permit rapid cell infiltration (Figure

2b). Also, by virtue of being made from gelatin (a hydrolyzed form of collagen), this gelatin scaffold presents binding motifs for cell binding, motility, and spreading.[28,29] For the inner compartment, we utilized a biphasic ferrogel with an Fe_3O_4-laden region on the top half of the cylindrical gel and an Fe_3O_4-free, porous, and deformable region on the bottom (Figure 2.c).

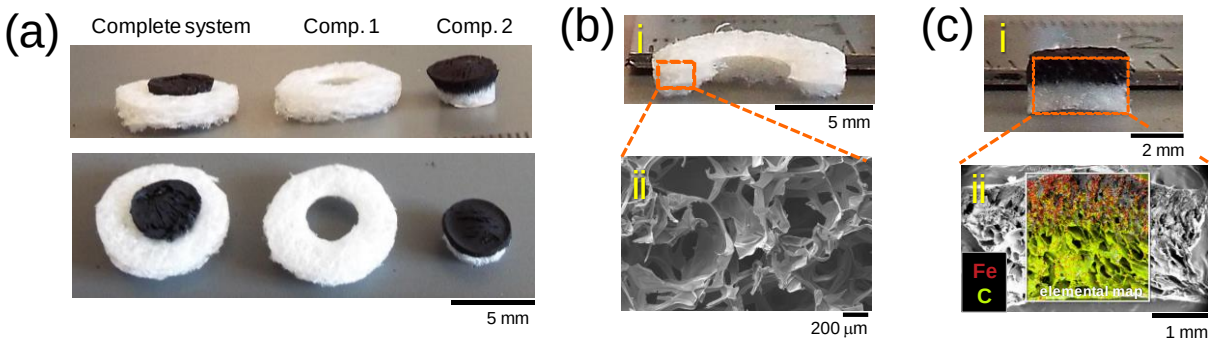

Figure 0.2. Two-compartment biomaterial system comprises a magnetically responsive biphasic ferrogel nested within an outer macroporous gelatin scaffold. (a) Photographs of the 2-compartment biomaterial system at an angle (top) and from the top (bottom). (b) Cross-sectional photograph (i) and SEM micrographs (ii) of the outer porous gelatin compartment. (b) Cross-sectional photograph (i) and SEM microgarphs (ii) of the inner biphasic ferrogel compartment. Elemental map reveals the location of iron (red) and carbon (yellow-green).

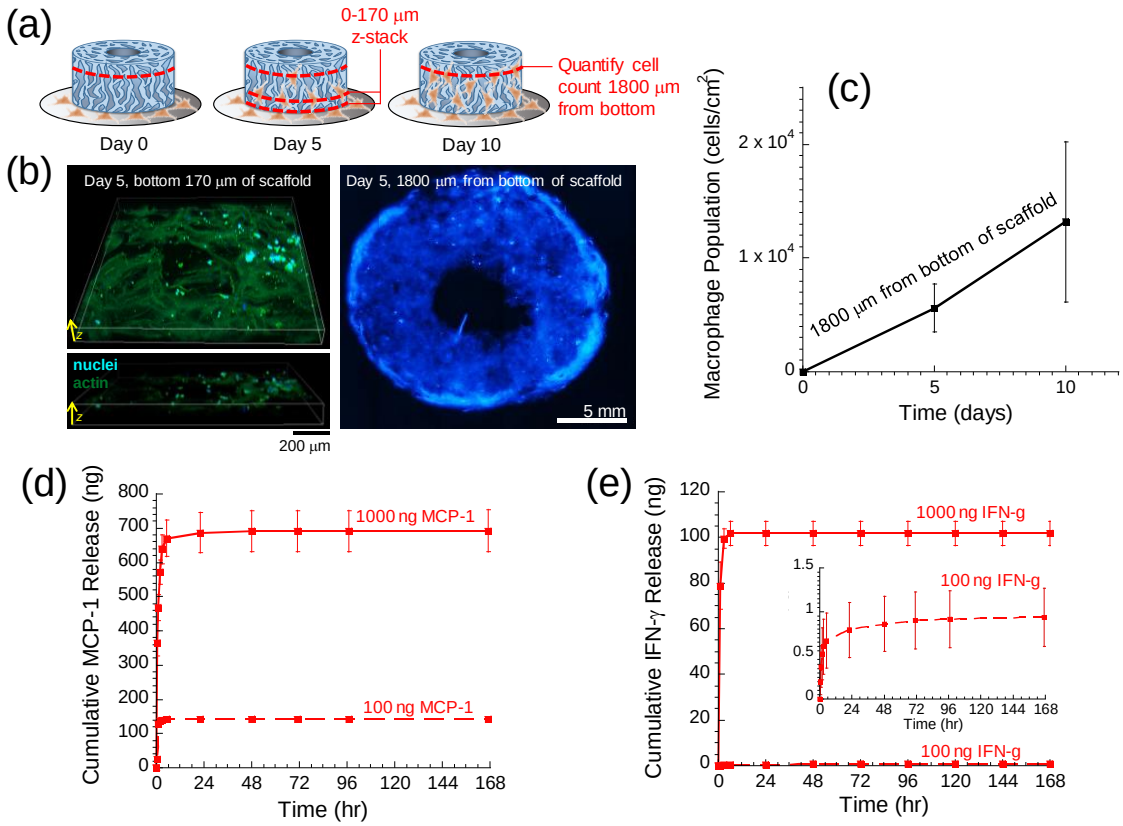

Figure 0.3. The outer macroporous gelatin scaffold can recruit and harbor macrophages and can rapidly release pro-inflammatory cytokines. (a) Schematic detailing how macrophages were recruited to the gelatin scaffold and where in the scaffold different images and measurements were taken. (b) Left: 3D z-stack detailing DAPI- (blue) and Phalloidin- (green) stained macrophages in the bottom 170 μm of the scaffold on day 5. Right: collage image of DAPI-stained macrophages (blue) taken 1800 μm from the bottom of the gel (200 μm from the top). (c) Quantification of macrophage density vs. time recorded 1800 microns from the bottom of the scaffold. (d) Cumulative release vs. time for scaffolds loaded with 1000 ng (solid) and 100 ng (dashed) of MCP-1. (e) Cumulative release vs. time for scaffolds loaded with 1000 ng (solid) and 100 ng (dashed) of IFN-γ. Inset: zoomed-in cumulative release vs. time for scaffold loaded with 100 ng IFN-γ. Parts (c)-(e), N = 4.

These biphasic ferrogels were designed to efficiently deform in the presence of a graded magnetic field (i.e., in the presence of fields emanating from simple hand-held

magnets or electromagnets). When magnetically deformed, these gels would release molecular payloads stored in the Fe_3O_4-free region in a magnetically triggered manner. The particular ferrogel formulation adopted here (1 wt% alginate, 7 wt% Fe_3O_4, 2.5 mM adipic acid dihydrazide cross-linked, freeze-dried at -20ºC) was previously shown to be optimal in terms of providing magnetically triggered deliveries.[30,31]

The outer porous gelatin scaffold was designed to provide initial deliveries of pro-inflammatory cytokines and to recruit and permit the residence of macrophages. To test this compartment's ability to recruit and establish macrophage populations, RAW 264.7 macrophages were seeded at 10,000 cells per well in a 12-well plate on Day -1 and allowed to establish themselves for 24 hours as a 2-dimensional (2D) colony. Then (at Day 0), gelatin scaffolds (compartment 1, Figure 2.b) were placed on top of 2D macrophage colonies and left for 10 days so that macrophages could infiltrate the volume of the scaffold (Figure 3a). On Day 5, some scaffolds were removed, fixed, and stained for f-actin (FITC-Phalloidin) and nuclei (DAPI), revealing that macrophages had infiltrated and spread within the bottom volume of the gel (Figure 3.b (left) and MovieS1.mov in Supporting Information). Also, by Day 5, some Macrophages had reached the top of the gel (Figure 3.b (right))). DAPI-stained macrophages residing 1800 μm from the bottom of the gel (i.e., 200 μm from the top of the 2-mm gel) were quantified using fluorescence microscopy on days 5 and 10 (Figure 3.c). This demonstrated that the macrophage populations could establish themselves and increase in population through the volume of these scaffolds over the course of 10 days in vitro. It must be noted that these in vitro studies utilized RAW macrophages which are more proliferative than the native macrophages that would be recruited to this material in vivo.

Thus, there is no way of knowing if macrophage population increase vs. time is due to migration through the material, proliferation, or some combination thereof. Additionally, the cell densities vs. time observed here (Figure 3.c) are likely higher than what would be expected in vivo. However, to enhance macrophage populations, these scaffolds could also be loaded with cytokines that could potentially expedite macrophage recruitment, as well as polarize them towards M1 phenotypes at early timepoints after implantation (e.g., MCP-1 and IFN-γ, respectively). These cytokines released rapidly at early time points (Figure 3.d & 3.e) due to excess cytokine being added to the outer compartment without rinsing off that excess cytokine prior to use. The total amount of cytokine delivered could be dictated simply by loading the scaffold with more or less cytokine (Figure 3.d & 3.e, comparing solid and dashed curves). Independent of loading, pro-inflammatory cytokine release ceased after roughly 12 hours (Figure S1), well before the times at which magnetic stimulation would be applied to trigger subsequent deliveries of anti-inflammatory cytokines.

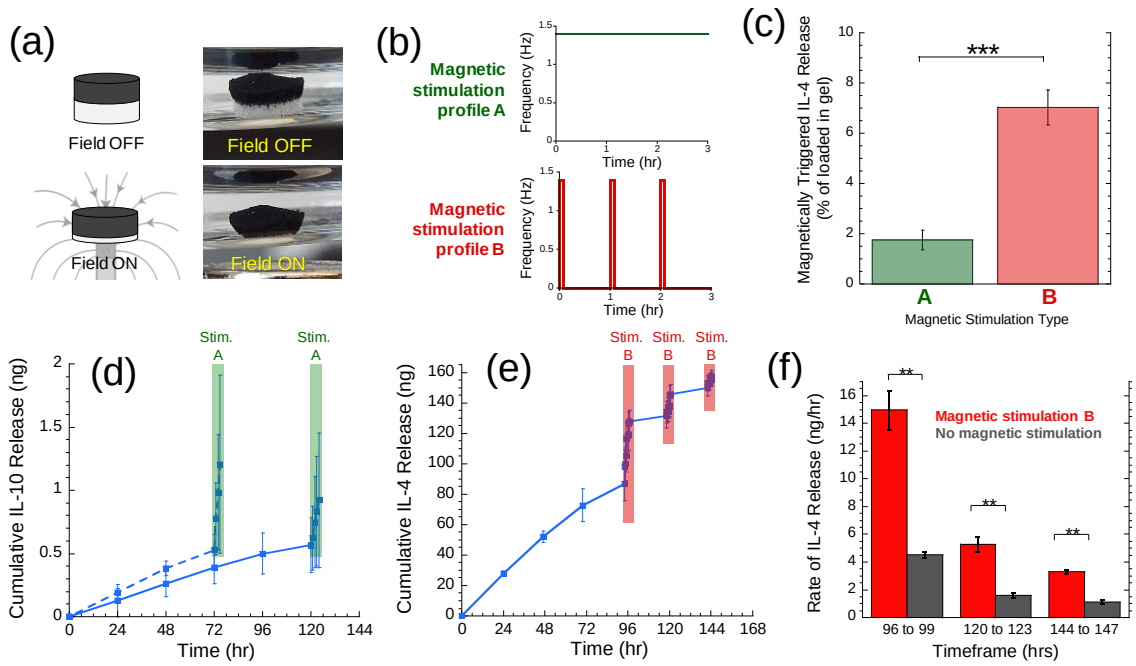

Figure 0.4. The inner ferrogel compartment can produce delayed, magnetically triggered anti-inflammatory cytokine delivery profiles. (a) Illustration (left) and photographs (right) of a biphasic ferrogel before (top) and during (bottom) magnetic compression. (b) Schematics of the two magnetic stimulation profiles used in these studies: (top, green) a cyclic magnetic field of 1.4 compressions per second continuously over 3 hours and (bottom, red) the same exposure but pulsed so that gels are cyclically compressed for 5 minutes every hour. (c) Amount released after 3 hours of stimulation profile A (green) vs. B (red). (d) Cumulative IL-4 release vs. time from ferrogels that were either magnetically stimulated on day 3 (dashed) or day 5 (solid). (e) Cumulative IL-10 release vs. time from ferrogels that were magnetically stimulated on days 4, 5, and 6. (f) Release rates over the indicated times when magnetically stimulated (red) vs. unstimulated (gray). For parts (c)-(f), ** and *** indicate statistically significant differences with $p < 0.01$ and 0.001, respectively (N = 4).

The inner compartment of this biomaterial system (Figure 2.c) was designed to provide delayed, on-demand, and magnetically triggered delivery of anti-inflammatory cytokines (e.g., IL-4 and IL-10). These biphasic ferrogels were designed so that cytokines could be loaded in their Fe_3O_4-free regions and released in earnest when magnetic gradients were used to compress the Fe_3O_4-free regions (Figure 4.a, white region of ferrogel compresses when a hand-held magnetic is subjacently applied). See

MovieS2.mov in Supporting Information for a movie of a biphasic ferrogel being magnetically compressed repeatedly at 1.4 Hz. Cytokine release rates prior to magnetic stimulation were kept at low levels by thoroughly rinsing ferrogels, as to remove excess cytokines that were not well-incorporated. Additionally, cytokine retention prior to magnetic stimulation was likely aided by the use of alginate as the polymeric constituent of these ferrogels. Alginate is heparin-mimicking, and heparin is known to bind strongly to a wide variety of cell-secreted proteins. In these studies, magnetic gradients were applied over the course of 3 hours, but with different temporal profiles (Figure 4.b): (i) one where a magnetic gradient was applied at a rate of 1.4 Hz continuously over 3 hours (Stimulation Profile A, top, green) and (ii) one where a magnetic gradient was applied at a rate of 1.4 Hz intermittently, lasting for 5 minutes every hour for 3 hours (Stimulation Profile B, bottom, red). The intermittent Profile B actually yielded higher rates of cytokine delivery compared to the continuous Profile A (Figure 4c). This is possibly due to the fact that magnetic compression results in release of molecules primarily contained in the macropore space and not contained in the gel's matrix (note that the Fe_3O_4-free region of these ferrogels are highly macroporous (Figure 2.c)). Thus, continuous 1.4 Hz stimulation (Profile A) may initially purge these more available molecules from the pore space but may prohibit the molecules in the gel from equilibrating (i.e., molecules that were purged from the macropore space cannot be replaced by molecules contained in the matrix space due to constant 1.4 Hz gel compression). This would result in a relatively low rate of release when averaged over 3 hours. However, intermittent stimulation (i.e., Stimulation Profile B) likely permits this re-equilibrium of molecules in the 1 hour between subsequent magnetic compressions, resulting in a distribution of molecules from

the matrix to the pore space. When magnetic stimulation continues, these relocated pore-space-molecules are efficiently purged. This may result in higher release rates when averaged over 3 hours. While these dynamics are outside the scope of this study, Stimulation Profile B has significant practical advantages in that it both produces higher rates of release and would be easier to implement *in vivo*. That is, 5 minutes of 1.4 Hz stimulation every hour can be implemented by manually brining a hand-held magnet close to the implant site whereas 3 hours of continuous 1.4 Hz stimulation could be tiring if performed manually. Nevertheless, neither magnetic stimulation profile resulted in statistically significant changes in gel mechanics (Figure S2), suggesting that magnetic stimulation does not overly damage the gels. This leaves open the possibility of magnetically stimulating at later time points for subsequent release busts.

Even though, Stimulation Profile A produced lower rates of release than Stimulation Profile B, it was nonetheless sufficient to significantly impact an anti-inflammatory cytokine's release profile. When loaded with 500 ng of IL-10, ferrogels released baseline levels of IL-10 prior to day 3 but dramatically increased release rates on day 3 when stimulated using Magnetic Stimulation Profile A (Figure 4.d, dashed curve). If this delayed IL-10 release was desired on day 5 rather than 3, magnetic stimulation could be applied on day 5 rather than day 3 (Figure 4.d, solid curve). This ability to control the time at which anti-inflammatories are earnestly released could provide a powerful tool for investigating how the duration of the inflammatory response impacts wound healing outcome. Magnetic stimulation can also potentially be used to repetitively deliver anti-inflammatory cytokines on subsequent days to prevent an inflammatory response from resurging. For example, when loaded with 1000 ng of IL-4, baseline levels

of IL-4 were released prior to magnetic stimulation. But, release rates were dramatically enhanced when stimulated on day 4 using Stimulation Profile B (Figure 4.e, compare slope of curve before 96 hours to the slope from 96 to 99 hours). The rate of IL-4 release could be subsequently enhanced on days 5 and 6 when magnetically stimulated on those days (Figure 4.e, enhanced slopes at 120 and 144 hours). These magnetically stimulated release rates on days 4, 5, and 6 were significantly higher than control gels upon which no magnetic stimulation was applied (Figure 4.f). These studies demonstrate our ability to control the timing and rate of these anti-inflammatory cytokine deliveries in an on-demand, magnetically prescribed manner.

The described biomaterial system could improve control over the inflammatory response in wound healing applications by locally regulating macrophage phenotype through carefully timed immunomodulatory cytokine deliveries. There is a growing preponderance of evidence suggesting that regulating macrophage phenotype vs. time is critical to achieving desired outcomes in wound healing and regenerative therapies,[32–36] and that sequenced deliveries of immunomodulatory cytokines can provide a means for this temporal regulation.[26,37] In fact, previous studies have designed scaffolding materials to release pro- and anti-inflammatory cytokines at different rates in an attempt to temporally control macrophage phenotype.[19,38–41] While these studies yielded promising results in their ability to influence macrophage phenotype in vivo, statistically significant improvements in regeneration were not observed (e.g., larger or more well-organized vessels/tissues). This could have been due to the inability to explicitly alter and optimize the timing of different cytokine deliveries (i.e., having the delay time of anti-inflammatory cytokines be a variable parameter between conditions). The biomaterial

system described here could enable explicit control over the timing of these deliveries, without having to alter the chemistry or structure of the implantable scaffold material between experiments. It should be noted, however, that with this material system's current formulation, macrophages initially recruited to the outer compartment may be exposed to baseline levels of anti-inflammatory cytokines diffusing out of the inner ferrogel (Figure. 4.d & 4e, IL-10 and IL-4 release is non-zero prior to magnetic stimulation). Even though magnetically stimulated release is significantly higher than diffusive release (Figure 4.d & 4.e, comparing slopes of curves with and without magnetic stimulation), if diffusive release establishes a bioactive concentration of anti-inflammatory cytokines, macrophages may begin to polarize towards pro-healing phenotypes prior to magnetic stimulation. Thus, fine-tuning of the biomaterial system will be required so that rates of release prior to magnetic stimulation result in sub-bioactive anti-inflammatory cytokine concentrations and release rates during magnetic stimulation result in bioactive concentrations. Such fine tuning can be achieved by modifying cytokine loading and ferrogel formulation (e.g., porosity, polymer concentration, polymer type, crosslinking density). Such a tuned biomaterial system will need to be tested in order to verify that this material system is capable of temporally regulating macrophage phenotype through magnetic stimulation.

In sum, we have developed a biomaterial system capable of initially delivering pro-inflammatory cytokines (MCP-1 and IFN-γ) from a macroporous gelatin structure capable of facilitating macrophage infiltration and growth. The amount of inflammatory cytokine release was dependent on the amount of cytokine loaded in the structure. This biomaterial system was also integrated with a biphasic ferrogel that was capable of

delivering anti-inflammatory cytokines (IL-4 and IL-10) in a delayed and magnetically triggered manner, using common hand-held magnets. The rate of magnetically stimulated delivery could be regulated by using different magnetic stimulation profiles and the timing of delivery could be regulated simply by choosing when to apply magnetic stimulation. This biomaterial system thus has the potential to enable experimental investigations into how the rate and timing of pro- and anti-inflammatory cytokine deliveries impact biological process critical in wound healing applications. Finally, this material system could also provide the material means to therapeutically implement optimized sequential cytokine deliveries, while retaining a high degree of clinical adaptability by enabling real-time alterations in delivery profiles.

Supporting Information: Appendix A

Additional experimental details and supplemental figures are provided in Supporting Information in Appendix A.

3.5 Acknowledgements

This work was funded by a Medical Research Grant from the Rhode Island Foundation (20144262), an Early Career Development Award from the Rhode Island IDeA Network of Biomedical Research Excellence (RI-INBRE, NIH/NIGMS 2P20GM103430), a 3M Company Non-Tenure Faculty Award (32976949), a grant from the National Science Foundation (NSF-CBET 1063433), and a NSF RII Track-2 FEC grant (NSF-1539068). The authors would like to thank Everett Crisman at the RI consortium for Nanoscience & Nanotechnology for help with SEM imaging and Al Bach and Kim Andrews in the RI-INBRE Centralized Research Core Facility for help with confocal microscopy imaging.

3.6 References

1. Sen CK, Gordillo GM, Roy S, et al. Human Skin Wounds: A Major and Snowballing Threat to Public Health and the Economy. *Wound Repair Regen*. 2010;17(6):763-771. doi:10.1111/j.1524-475X.2009.00543.x.Human
2. Stojadinovic A, Carlson JW, Schultz GS, Davis TA, Elster EA. Topical advances in wound care ☆. *Gynecol Oncol*. 2008;111(2):S70-S80. doi:10.1016/j.ygyno.2008.07.042
3. J. SA, A.F. CR. Cutaneous Wound Healing. *N Engl J Med*. 1999;341(10):738-746. doi:10.1056/NEJM199909023411006
4. Boateng JS, Matthews KH, Stevens HNE, Eccleston GM. Wound healing dressings and drug delivery systems: a review. *J Pharm Sci*. 2008;97(8):2892-2923. doi:10.1002/jps.21210
5. Velnar T, Bailey T, Smrkolj V. The wound healing process: an overview of the cellular and molecular mechanisms. *J Int Med Res*. 2009;37(5):1528-1542.
6. Moura LIF, Dias AMA, Carvalho E, De Sousa HC. Recent advances on the development of wound dressings for diabetic foot ulcer treatment - A review. *Acta Biomater*. 2013;9(7):7093-7114. doi:10.1016/j.actbio.2013.03.033
7. Frykberg RG, Banks J. Challenges in the Treatment of Chronic Wounds. *Adv wound care*. 2015;4(9):560-582. doi:10.1089/wound.2015.0635
8. Blakytny R, Jude E. The molecular biology of chronic wounds and delayed healing in diabetes. *Diabet Med*. 2006;23(6):594-608. doi:10.1111/j.1464-5491.2006.01773.x

9. Buckley CD, Gilroy DW, Serhan CN, Stockinger B, Tak PP. The resolution of inflammation. *Nat Rev Immunol*. 2013;13(1):59-66. doi:10.1038/nri3362

10. Eming SA, Krieg T, Davidson JM. Inflammation in Wound Repair: Molecular and Cellular Mechanisms. *J Invest Dermatol*. 2007;127(3):514-525. doi:10.1038/sj.jid.5700701

11. Werner S, Grose R. Regulation of wound healing by growth factors and cytokines. *Physiol Rev*. 2003;83(3):835-870. doi:10.1152/physrev.00031.2002

12. Martinez FO, Helming L, Gordon S. Alternative Activation of Macrophages: An Immunologic Functional Perspective. *Annu Rev Immunol*. 2009;27(1):451-483. doi:10.1146/annurev.immunol.021908.132532

13. Park JE, Barbul A. Understanding the role of immune regulation in wound healing. *Am J Surg*. 2004;187(5 SUPPL. 1):S11-S16. doi:10.1016/S0002-9610(03)00296-4

14. Van Amerongen MJ, Harmsen MC, Van Rooijen N, Petersen AH, Van Luyn MJA. Macrophage depletion impairs wound healing and increases left ventricular remodeling after myocardial injury in mice. *Am J Pathol*. 2007;170(3):818-829. doi:10.2353/ajpath.2007.060547

15. Wynn TA, Chawla A, Pollard JW. Macrophage biology in development, homeostasis and disease. *Nature*. 2013;496(7446):445-455. doi:10.1038/nature12034

16. Martinez FO, Sica A, Mantovani A, Locati M. Macrophage activation and polarization. *Front Biosci*. 2008;13:453—461. doi:10.2741/2692

17. Kim YH, Furuya H, Tabata Y. Enhancement of bone regeneration by dual release of a macrophage recruitment agent and platelet-rich plasma from gelatin hydrogels.

Biomaterials. 2014;35(1):214-224. doi:10.1016/j.biomaterials.2013.09.103

18. Kumar VA, Taylor NL, Shi S, Wickremasinghe NC, D'Souza RN, Hartgerink JD. Self-assembling multidomain peptides tailor biological responses through biphasic release. *Biomaterials*. 2015;52(1):71-78. doi:10.1016/j.biomaterials.2015.01.079
19. Spiller KL, Nassiri S, Witherel CE, et al. Sequential delivery of immunomodulatory cytokines to facilitate the M1-to-M2 transition of macrophages and enhance vascularization of bone scaffolds. *Biomaterials*. 2015;37:194-207. doi:10.1016/j.biomaterials.2014.10.017
20. Julier Z, Park AJ, Briquez PS, Martino MM. Promoting tissue regeneration by modulating the immune system. *Acta Biomater*. 2017;53:13-28. doi:10.1016/j.actbio.2017.01.056
21. Koh TJ, DiPietro LA. Inflammation and wound healing: the role of the macrophage. *Expert Rev Mol Med*. 2011;13(July):1-12. doi:10.1017/S1462399411001943
22. Vishwakarma A, Bhise NS, Evangelista MB, et al. Engineering Immunomodulatory Biomaterials To Tune the Inflammatory Response. *Trends Biotechnol*. 2016;34(6):470-482. doi:10.1016/j.tibtech.2016.03.009
23. Lin CC, Metters AT, Anseth KS. Functional PEG-peptide hydrogels to modulate local inflammation inducedby the pro-inflammatory cytokine TNFα. *Biomaterials*. 2009;30(28):4907-4914. doi:10.1016/j.biomaterials.2009.05.083
24. Lin CC, Boyer PD, Aimetti AA, Anseth KS. Regulating MCP-1 diffusion in affinity hydrogels for enhancing immuno-isolation. *J Control Release*. 2010;142(3):384-391. doi:10.1016/j.jconrel.2009.11.022

25. Kajahn J, Franz S, Rueckert E, et al. Artificial extracellular matrices composed of collagen I and high sulfated hyaluronan modulate monocyte to macrophage differentiation under conditions of sterile inflammation. *Biomatter*. 2012;2(4):226-236. doi:10.4161/biom.22855

26. Pajarinen J, Tamaki Y, Antonios JK, et al. Modulation of mouse macrophage polarization in vitro using IL-4 delivery by osmotic pumps. *J Biomed Mater Res - Part A*. 2015;103(4):1339-1345. doi:10.1002/jbm.a.35278

27. Martinez FO, Gordon S. The M1 and M2 paradigm of macrophage activation: time for reassessment. *F1000Prime Rep*. 2014;6(March):1-13. doi:10.12703/P6-13

28. Van Den Steen PE, Dubois B, Nelissen I, Rudd PM, Dwek RA, Opdenakker G. *Biochemistry and Molecular Biology of Gelatinase B or Matrix Metalloproteinase-9 (MMP-9)*. Vol 37.; 2002. doi:10.1080/10409230290771546

29. Gomez-Guillen MC, Gimenez B, Lopez-Caballero ME, Montero MP. Functional and bioactive properties of collagen and gelatin from alternative sources: A review. *Food Hydrocoll*. 2011;25(8):1813-1827. doi:10.1016/j.foodhyd.2011.02.007

30. Zhao X, Kim J, Cezar C a, et al. Active scaffolds for on-demand drug and cell delivery. *Proc Natl Acad Sci U S A*. 2011;108(1):67-72. doi:10.1073/pnas.1007862108

31. Cezar C a, Kennedy SM, Mehta M, et al. Biphasic Ferrogels for Triggered Drug and Cell Delivery. *Adv Healthc Mater*. 2014:1-8. doi:10.1002/adhm.201400095

32. Brown BN, Valentin JE, Stewart-Akers AM, McCabe GP, Badylak SF. Macrophage phenotype and remodeling outcomes in response to biologic scaffolds with and without a cellular component. *Biomaterials*. 2009;30(8):1482-1491.

doi:10.1016/j.biomaterials.2008.11.040

33. Badylak SF, Valentin JE, Ravindra AK, McCabe GP, Stewart-Akers AM. Macrophage Phenotype as a Determinant of Biologic Scaffold Remodeling. *Tissue Eng Part A*. 2008;14(11):1835-1842. doi:10.1089/ten.tea.2007.0264

34. Langer R, Tirrell DA. Designing materials for biology and medicine. *Nature*. 2004;428(6982):487-492. doi:10.1038/nature02388

35. Roh JD, Sawh-Martinez R, Brennan MP, et al. Tissue-engineered vascular grafts transform into mature blood vessels via an inflammation-mediated process of vascular remodeling. *Proc Natl Acad Sci*. 2010;107(10):4669-4674. doi:10.1073/pnas.0911465107

36. Diegelmann, Robert F; Evans MC. Wound healing: an overview of acute, fibrotic and delayed healing. *Front Biosci*. 2004;9(1):283-289.

37. Garash R, Bajpai A, Marcinkiewicz BM, Spiller KL. Drug delivery strategies to control macrophages for tissue repair and regeneration. *Exp Biol Med*. 2016;241(10):1054-1063. doi:10.1177/1535370216649444

38. Keeler GD, Durdik JM, Stenken JA. Acta Biomaterialia Localized delivery of dexamethasone-21-phosphate via microdialysis implants in rat induces M (GC) macrophage polarization and alters CCL2 concentrations. *Acta Biomater*. 2015;12:11-20. doi:10.1016/j.actbio.2014.10.022

39. Reeves, Andrew RD, Kara L. Spiller, Donald O. Freytes, Gordana Vunjak-Novakovic and DLK. Controlled Release of Cytokines Using Silk-biomaterials for Macrophage Polarization. *Biomaterials*. 2015;344(6188):1173-1178. doi:10.1126/science.1249098.Sleep

40. Chung ES, Chauhan SK, Jin Y, et al. Contribution of macrophages to angiogenesis induced by vascular endothelial growth factor receptor-3-specific ligands. *Am J Pathol*. 2009;175(5):1984-1992. doi:10.2353/ajpath.2009.080515

41. Spiller KL, Anfang RR, Spiller KJ, et al. The role of macrophage phenotype in vascularization of tissue engineering scaffolds. *Biomaterials*. 2014;35(15):4477-4488. doi:10.1016/j.biomaterials.2014.02.012

Chapter 4

Manuscript (II): Magnetically responsive biomaterial system enables on-demand, sequential delivery of biomolecules for variety of biomedical applications.

In preparation for submission to *ACS Science and Engineering Journal*

By Anita E. Tolouei, Tania T. Emi, Zahra M. Madani, Stephen Kennedy*

Department of Chemical Engineering,

University of Rhode Island, Kingston, Rhode Island 02881

* Corresponding author: Stephen Kennedy

Email: smkennedy@uri.edu,

Phone: (401) 874-5295,

Fax: (401) 782-6422

4.1 Abstract

Sequential protein release is required in regulating many biological processes that underlie injury and disease. A magnetically responsive dual-compartment biomaterial was therefore designed and successfully applied to provide on-demand sequential release of proteins relevant to specific therapies that would benefit from sequential release. The composition of this biomaterial system consists of a gelatin outer compartment and a ferrogel inner compartment. Three pairs of relevant proteins were incorporated in the biomaterial system: (1) Granulocyte-Macrophage Colony-Stimulating Factor (GM-CSF, a dendritic cell recruitment factor) and Heat Shock Protein 27 (HSP27, as a model cancer antigen) for use in cancer immunotherapy; (2) Vascular Endothelial Growth Factor (VEGF, an angiogenic sprouting factor) and Platelet Derived Growth Factor (PDGF, a factor that aids in maturing vascular sprouts) for tissue vascularization; and, (3) Stromal cell Derived Factor-1α (SDF-1α, a bone progenitor cell recruitment factor) and bone morphogenetic protein 2 (BMP2, a osteo-differentiation factor) for bone regeneration. It was demonstrated that proteins loaded in the outer compartment (GM-CSF, VEGF, SDF-1α) released rapidly within the first 24 to 100 hours and that the amount released was dependent on how much protein was loaded in the compartment. timing and rate of release of these proteins can be controlled via magnetic stimulation. Proteins loaded in the inner ferrogel (HSP27, PDGF, BMP2) could be magnetically triggered to provide delayed enhancements in release rate where the timing (between days 1 and 8) and rate of release (0.2 to 1 ng/hr) were externally controlled through the temporal profile of magnet application and the frequency of that application. This biomaterial system can be used to investigate how the timing and sequence of protein deliveries impacts the biological

processes that underlie cancer immunotherapy, tissue vascularization, and bone regeneration (and potentially in many other therapeutic areas) and can be used to experimentally optimize deliveries in these therapies.

4.2 Introduction

Hydrogels have been commonly used as biomaterials in drug delivery and tissue engineering applications due to their biocompatibility and versatility. [1–3] These drug delivery materials can potentially control important biological processes that need to be regulated to treat injury and disease. However, most biologies are sequential in nature and require sequential presentations of bio-instructive factors for proper regulation. For example, cancer is the second most common cause of death in the United States and accounts for nearly 1 of every 4 deaths.[4] This emphasizes the necessity of finding effective cancer treatment strategies. One promising cancer treatment strategy is biomaterials-based immunotherapy in which the immune system of the patient's own body is reprogramed in order to initiate an immunological attack against cancer cells.[5–7] In this approach, first, dendritic cells (DCs) need to be recruited to the biomaterial by releasing a DC recruitment factor (Factor I) (Fig 1.A.i, ii). Once a large number of DCs are resident in the biomaterial (Fig 1.A.iii), they can become activated when presented with a cancer antigen (Factor II) (Fig 1.A.iv). Activated DCs would then migrate out of the biomaterial towards lymph node (Fig 1.A.v), triggering an immunological attack against cancer. Therefore, sequential release of recruitment factor followed by release of activating factor could potentially improve control over regulating the biological processes pertinent to biomaterial-based cancer immunotherapies.

Beyond cancer treatments, regulation of vascular growth can be of great potential in the treatment of different cardiovascular diseases (CVDs), which are the most common cause of death in the United States and worldwide.[8] It has been reported that CVD was the main cause of more than 50% of deaths in 2010.[9] Additionally, regeneration of tissues after surgery or injury often involves regulating the growth of new vascular networks.[10–12] Pericyte cells play a key role in vessel formation and presentation of several growth factors can regulate this process.[13] For example, growth of new blood vessels can be initiated by an initial presentation of angiogenic factors (Factor I) which instructs pericyte cells to detach from the endothelium of nearby vasculature. This detachment destabilizes the endothelium and allows small vascular sprouts to grow away from the existing blood vessel (Fig 1.B.i, ii). These nascent sprouts are thin, unorganized, and not mature enough to efficiently perfuse blood through them (Fig 1.B.iii). Hence, an additional maturation factor (Factor II) is subsequently released to recruit pericyte cells back to neovessels (Fig 1.B.iv), which in turn helps neovessels mature into a thicker and more interconnected network (Fig 1.B.v).

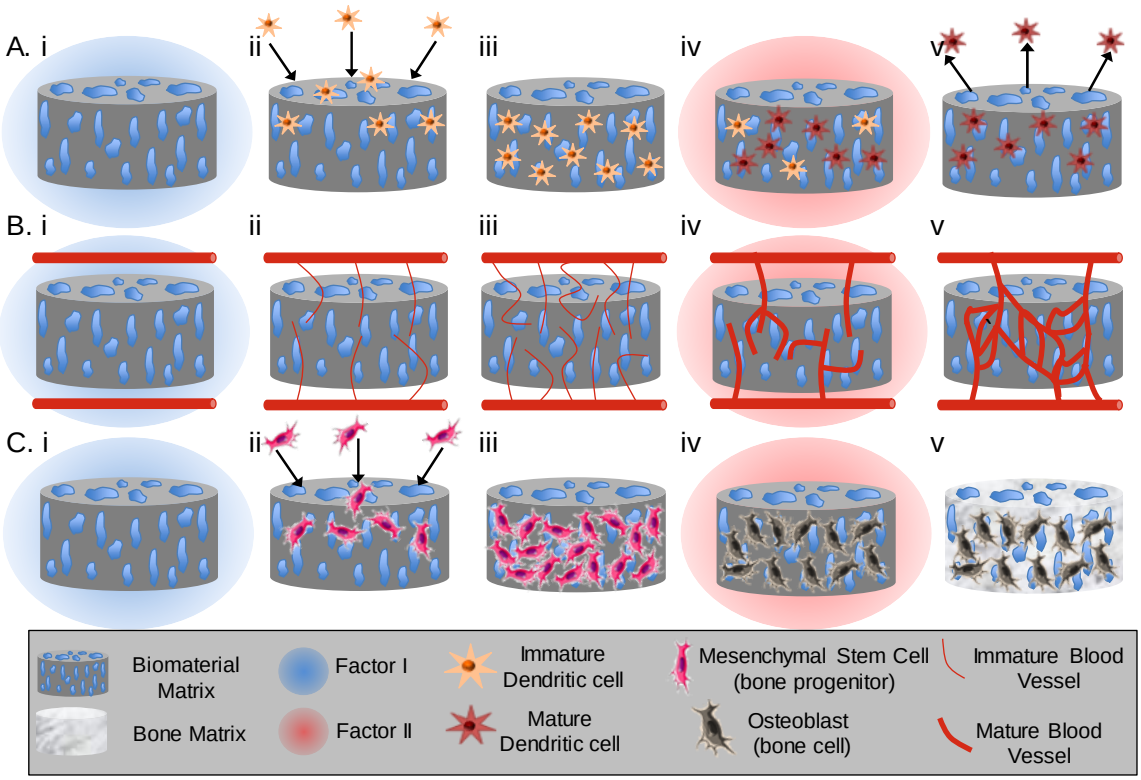

Figure 0.1. Sequential delivery of multiple factors is essential for improved outcome in multiple therapies. A) Schematic showing how sequenced deliveries could be beneficial for biomaterial-based cancer immunotherapy B) tissue vascularization and C) bone regeneration.

Finally, sequential delivery of bio-instructive factors can be of potential value in regenerating bone tissues. Each year more than 6 million bone fractures occur in the United States, leading to approximately 900,000 patient hospitalizations.[14] Biomaterial scaffolds can be promising substitutes for traditional autogenic and allogenic grafting since they can decrease the problems associated with donor site sensitivity, morbidity, and limited availability of these grafts.[15,16] Bone regeneration also is naturally regulated by a sequence of growth factor presentations.[17] First, osteoprogenitor cells need to be recruited to the scaffold by releasing a bone progenitor recruitment factor (Factor I) (Fig 1.C.i, ii). After establishing a population of these progenitor cells in the biomaterial (Fig

1.C.iii), they can be differentiated down the osteogenic lineage by exposing them to a osteo-differentiation factor (Factor II) (Fig 1.C.iv). Differentiated bone cells would then start secreting their own robust bone matrix, which is a vital step in regenerating new bone tissues (Fig 1.C.v).Therefore, in order to better regulate these regenerative processes, sequential delivery of bone progenitor recruitment and differentiation factors is necessary.

In previous studies, hydrogels were demonstrated to have sequentially protein release capabilities using formulations containing phases with different degradation rates. However, the timing between these two deliveries was not capable of being regulated after implantation or injection of these biomaterials.[18–20] Additionally, these delivery profiles can more aptly be described as dual deliveries with different rates and not sequential release per se (i.e., on burst release followed by a second, delayed burst release). The biomaterial system presented here was specifically designed to provide sequential delivery profiles where there is an initial burst release of one factor followed by a magnetically triggered, delayed release of a second factor. This was achieved by composing the biomaterial with two compartments (Fig 2.A.i, ii). Compartment 1, initially releases Factor I and has a functionality to maintain recruited cells (Fig 2.A.iii, iv). Compartment 2 is capable of releasing Factor II in an on-demand manner when remotely stimulated with a magnetic field (Fig 2.A.v). This study aimed to demonstrate the ability to generate these sequential delivery profiles for specific recruitment factors (GM-CSF, VEGF, SDF-1α) followed by magnetically triggered delivery of programming factors (HSP27, PDGF, BMP2) (Figure 2.B), which are relevant to regulating sequential

biologies in cancer immunotherapy, generation of new vascular networks, and in regenerating bone tissues, respectively (Fig 2.C).

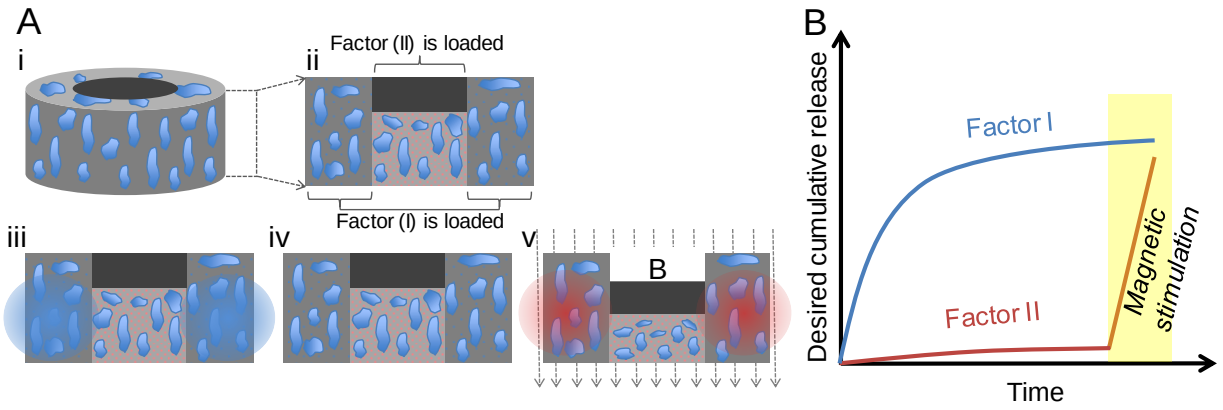

C

Goal	Factor 1	Factor 2
1. Cancer Immunotherapy	GM-CSF	HSP-27
2. Tissue Vascularization	VEGF	PDGF
3. Bone Regeneration	SDF1-α	BMP2

Figure 0.2. New Biomaterial system is designed to improve sequential delivery of several factors in an on-demand manner. A) Schematic of the multi-compartment biomaterial system shows how delivery of multiple factors can be accomplished in a controlled sequenced manner B) Desired cumulative release of factor I and II. C) Table shows different therapies and factors mediating these processes.

4.3 Materials and methods

4.3.1 Materials

High guluronate content sodium alginate (Protonal LF 20/40) with molecular weight of ~ 250 kDa was provided by Pronova Biopolymers (Olso, Norway). Other chemicals such as Adipic Acid Dihydrazide (AAD), 1-ethyl-3-(dimethylaminopropyl)

carbodiimide (EDC), compound 2-(N-morpholino)ethanesulfonic acid (MES), 1-hydroxybenzotriazole (HOBt), iron (II,III) oxide powder (< 5 micron), Phosphate Buffered Saline (PBS), Sigmacote®, and Bovine Serum Albumin (BSA) were all purchased from Sigma-Aldrich (St. Louis, MO). Granulocyte Macrophage Colony Stimulating Factor (GM-CSF), Heat shock Protein 27 (HSP27), Vascular Endothelial Growth Factor (VEGF), Platelet Derived Growth Factor (PDGF), Stromal Cell-derived Factor 1-α (SDF-1α), Bone Morphogenetic Protein 2, and all Enzyme-linked Immunosorbent Assay (ELISA) kits and kit reagents were purchased from R&D Systems (Minneapolis, MN). Lyophilized gelatin sponges (GelFoam™ sponge sheets) were purchased from Pfizer (Groton, CT).

4.3.2 Fabrication and characterization of biomaterial system

The outer compartments of these two-compartment biomaterial systems were made from GelFoam™ gelatin sponges. The 2 x 12 x 7 mm GelFoam™ lyophilized sheets provided by the manufacturer were shaped into hollow cylinders with biopsy punches (2 mm thick, 8 mm outer diameter-OD, 4 mm inner diameter-ID). In order to image the gel's porous structures, they were sputter-coated with gold for 30 seconds and imaged under the Scanning Electron Microscopy (SEM) on a Zeiss SIGMA VP Field Emission-SEM and Energy-dispersive X-ray Spectroscopy (EDS) for elemental mapping.

The inner compartment ferrogels were made of alginate according in a similar manner to the biphasic ferrogels described elsewhere.[21–23] Briefly, alginate (at 1%wt) was dissolved in MES buffer (100 mM MES and 500 mM NaCl at pH = 6.0) with AAD and HOBt. This mixture was then mixed with iron Oxide particles (Fe_3O_4 < 5 μm) and 100 mg/mL EDC. Next, the mixture was cast between two sigmacote-treated glass plates

separated by 2 mm spacers. During casting (~ 30 minutes), a magnet was placed on top of the glass plate to pull the iron oxides to the top of the ferrogel, resulting in a biphasic design. Ferrogels were then cut into 4 x 2 mm (diameter- thickness) disks using 4-mm biopsy punches. Gels were then washed in deionized water for 3 days with water being changed 2 to 3 times a day, this was done in order to remove residual reagents and let them swell. Next, to achieve a porous structure, gels were frozen overnight at -20 °C and lyophilized. For SEM imaging, ferrogels were cut with a sharp razor, exposing their cross section and prepped for SEM imaging following the same protocol as described above for gelatin outer compartments.

4.3.3 Magnetic stimulation of ferrogels

Two different set up were used to magnetically stimulate the Ferrogels, both involving the use of 0.5”x0.5” cylindrical neodymium magnets (K&J Magnetics, Pipersville, PA). In one apparatus, magnets were incorporated on a variable-speed laboratory rocker where magnets were placed on the edges of its platform (4 magnets on one edge and 4 on the opposite edge). Sigmacote-treated scintillation vials containing gels were placed on top of these magnets with aluminum clamps and suspended using standard aluminum laboratory scaffolding. The rocker platform positioned magnets close (~ 1 mm) to ferrogels contained in the suspended scintillation vials when in the upward position and positioned the magnets far from the ferrogels when in the downward position, thus magnetically stimulating the ferrogels in a cyclic manner. The frequency of the applied magnetic stimulation was thus dependent on the oscillation speed of rocker with 1.4 Hz being the maximum frequency produced from this apparatus (i.e., magnetic compression of the ferrogel at a rate of 1.4 Hz under a ~ 5 kGauss magnetic field). While

somewhat limited in the frequency of magnetic stimulation, this stimulation apparatus was capable of continuously stimulating 8 ferrogels simultaneously continuously for days.

A second apparatus was used for exposing ferrogels to slightly higher frequencies (up to 14 Hz) but for relatively short periods of time (see Emi et al. for a more thorough description[23]). This second setup consisted of a crankshaft driven by a programmable electric motor. The crankshaft was connected via cams to four pistons (much like a car engine) that would move up and down in a sinusoidal manner as the crankshaft was turned by the electric motor. Each piston contained a neodymium magnet and a scintillation vial containing a ferrogel could be suspended directly above each of the four pistons. Thus, when the piston was in the up position, a ferrogel would be exposed to a strong magnetic field (measured to be 5 kGauss). When the piston was in the down position, the magnetic field was weak (measured to be < 10 Gauss). Thus, the speed of the motor dictated the magnetic stimulation frequency. It was determined that this apparatus could magnetically stimulate ferrogels at frequencies up to 14 Hz.

4.3.4 Protein release studies

In order to load proteins to these gels, concentrated solutions of proteins in PBS were made. It was determined that each outer gelatin compartment had the capacity to absorb 40 μl of solution which was used as the basis to calculate protein loading concentrations (i.e., loading of 1000 ng protein would require preparation of a solution containing 1000 ng GM-CSF in 40 μl PBS). Sigmacote-treated scintillation vials (to prevent protein adsorption to the surface of the vials) were used as containers for these gels. Protein carrying solutions were added dropwise to these outer compartments for

loading. Vials were capped, and gels were left at room temperature overnight for full absorption of the protein into the gels. Release studies began the next day when gels were submerged in PBS with 1% BSA (t = 0). 1 ml samples were collected periodically and replaced with fresh media each time. Collected samples were stored in 1.5 ml low-adsorption tubes in the freezer. After collecting all samples, samples were thawed and quantified for protein content (i.e., GM-CSF, VEGF, SDF-1α) using ELISA.

Inner compartment fabrication resulted in lyophilized alginate biphasic gels with a layer of iron-oxide-free porous alginate on one side of the gel and an iron-oxide saturated layer with smaller pores on the other side of the gel. The loading of these ferrogels and release studies from them were similar to those described for the outer gelatin compartments above. However, the absorption capacity of these ferrogels were 20 μl. Ferrogels were placed in scintillation vials with their iron-oxide free region facing up. Next, a 20 μl solution containing protein was added to them dropwise. Vials were capped and left in order for gels to absorb the proteins overnight. Ferrogels were flipped over so that their iron-oxide-saturated regions faced upwards (so that a magnet applied under the vial would deform the ferrogel in a downward motion) and then rinsed in PBS with 1% BSA for between 1 to 4 days to remove proteins that were not well integrated in the gel structure. Samples were then taken at different times and fresh media was replaced at each time point. During these time course release experiments, ferrogels were magnetically stimulated at a number of time points and at various frequencies, depending on the experiment. ELISA was performed on the collected samples to quantify the concentration of the released proteins from ferrogels (HSP27, PDGF, BMP2).

4.3.5 Data representation and statistical analysis

Analysis of variance (ANOVA) with post-hoc Tukey HSD (Honestly Significant Difference) test was performed in order to determine statistically significant differences when multiple conditions and comparison were made. The numerical values presented in the graphs were represent means ± standard deviations from 4 independent replicates (N = 4). P-values less than 0.05 were considered significant.

4.4 Results

4.4.1 Characterization of the two-compartment biomaterial system

The two-compartment biomaterial system was made of an outer gelatin compartment and an inner biphasic ferrogel nested within the outer gelatin compartment (Fig 3. A). The gelatin outer compartment was highly porous (Figure 3. B), which would be desirable for allowing fast diffusive release of load proteins (due to high surface area) and potentially efficient penetration of recruited cells. Additionally, by virtue of being made from gelatin, this outer compartment contained cell-binding integrins needed to have recruited cells attach the scaffold and proliferate within the scaffold. The inner biphasic ferrogel compartment contained a Fe_3O_4 saturated region on the one side of the gel and a highly porous Fe_3O_4-free region on the opposite side of the gel (Fig 3. C. i). This biphasic structure was capable of deforming in the presence of magnetic field (Fig 3. C. ii).

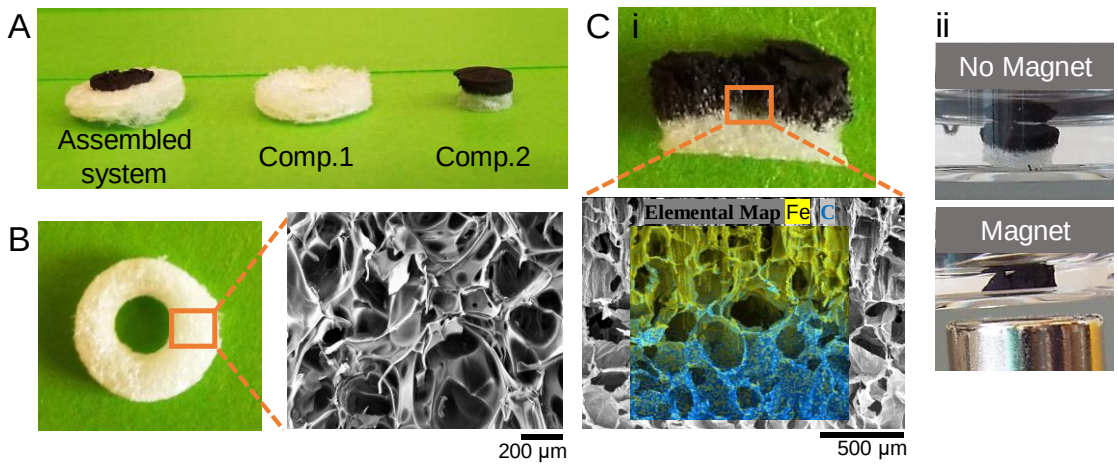

Figure 0.3. Dual Compartment biomaterial system with porous outer compartment and magnetically responsive inner compartment. A) Photographs of the whole system B) Characterization of the outer compartment with SEM imaging. C) i. SEM with elemental mapping (bottom) differentiates between Iron (yellow) and carbon (blue) parts of the gel. ii. Ferrogels before (top) and after (bottom) stimulating with magnet.

4.4.2 Release characteristics of the outer gelatin scaffold

The outer compartment's porous gelatin scaffold was capable of initially releasing proteins (proteins described herein as "Factor I") in a rapid manner. Specifically, DC recruitment factor (GM-CSF) released mostly within the first 24 hours (Figure 4. A). The total amount of GM-CSF release was dependent on the amount loaded in the outer compartment (Figure, 4. A: higher loadings resulted in higher amounts of cumulative release). This rapid and adjustable initial release of DC recruitment factor may be useful in rapidly recruiting DCs to the scaffold for biomaterials-based cancer immunotherapy applications. Similarly, pro-angiogenic factors (VEGF) rapidly released from the gelatin scaffold, depleting from the gel within the first 12 hours (Figure 4. B). VEGF cumulative release was also dependent on the amount loaded into the scaffold (Figure 4. B: higher loadings plateaued at higher levels of cumulative release). This rapidly release of VEGF may be useful in rapidly initiating vascular sprouting into the scaffold in applications that

demand neo-vascularization (e.g., treating CVDs, wound healing and tissue engineering applications). Finally, bone progenitor recruitment factor (SDF-1a) released in a relatively rapid manner, plateauing 200 hours (Figure 4. C). Again, the final cumulative release values were a function of the amount of protein loaded (Figure 4. C: higher loadings yielded higher plateau values). This relatively rapid release profile may enable rapid recruitment of bone progenitor cells to the scaffold for bone regeneration applications.

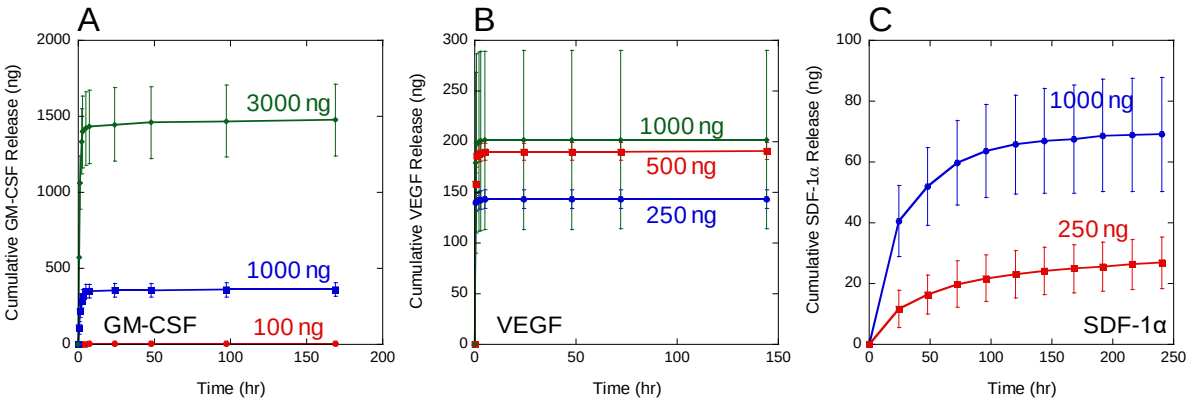

Figure 0.4. The outer compartment can rapidly release initial factors pertinent to cancer immunotherapy, tissue vascularization, and bone regeneration. A) Cumulative release versus time of GM-CSF, B) VEGF, and C) SDF-1α from outer compartment when loaded with different amounts of proteins (Colors represent different protein concentrations).

4.4.3 Release characteristics of the inner ferrogel

The inner compartment provides magnetically triggered, delayed, and on-demand release of proteins that can be used to direct the behavior of (i.e., program) cells recruited to the outer compartment. For example, a model cancer antigen's (HSP27's) release rate drastically increase when ferrogels inner compartments are magnetically stimulated on days 4 (Figure 5. A, slope of blue curve increases in the blue shaded region of the curve)

or on day 7 (slope of red curve increases in the red shaded region), depending on when the magnetic stimulation is applied (i.e., on day 4 or 7, respectively). Note that the magnetic stimulation used in these studies was at constant 1.4 Hz for 4 hours using the rocker. These on-demand, delayed enhancements in release rate could be used to optimize the timepoint at which recruited DCs are earnestly presented with cancer antigen for biomaterials-based cancer immunotherapy applications.

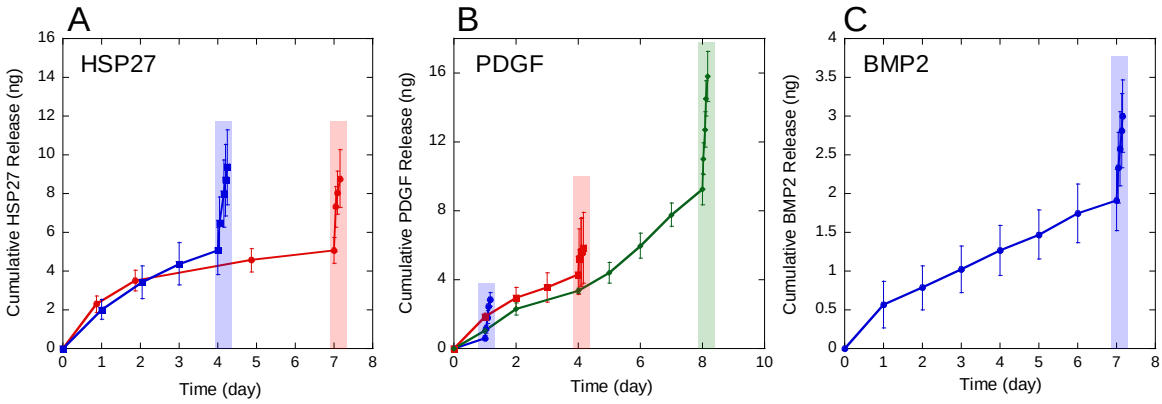

Figure 0.5. Timing of the delivery from ferrogels can be controlled by stimulating at different time points. A) Cumulative release of HSP27 when stimulated on days 4 (blue) and 7 (red). B) PDGF on days 1 (blue), 4 (red), 8 (green), and C) BMP2 on days 7 (blue).

Likewise, the rate of pro-vascular-maturation factor (PDGF) release could be greatly enhanced when these ferrogel inner compartments were magnetically stimulated (Figure 5. B). And again, the time at which magnetic stimulation was applied enabled this enhanced release to occur at specific times (Figure 5. B: magnetic stimulation on days 1 (blue), 4 (red), or 8 (green) yielded enhancements in release rates on days 1, 4, or 8, respectively). These magnetically triggered delays in pro-vascular-maturation factors could help optimize the time allotted for inducing vascular sprouting before re-stabilizing the nascent vascular network.

Finally, the rate of osteo-differentiation factor (BMP2) release could also be enhanced when these ferrogels were magnetically stimulated (Figure 5. C: increased slope of the blue curve in the blue shaded region). Though the specific timing of this magnetically triggered enhancement in release rate was not demonstrated as was with PEGF and HSP27, it is likely that enhancements in release would be generated at different time points upon magnetic stimulation at different time points. The ability to magnetically trigger enhancements in osteo-differentiation factors to recruited bone progenitors may allow for optimizations in how much time is provided to build bone progenitor populations in the scaffold prior to instructing them to differentiate.

4.4.4 Strategies for magnetically controlling the rate of delayed release

While the delayed release capabilities outlined above may be of use in improving the timing of deliveries in cancer immunotherapies, re-vascularization therapies, and bone regeneration, the rate of release when magnetically stimulated is also a critical parameter for optimization. Here, strategies were explored for using alterations in the magnetic stimulation profile to regulate the release rate during magnetic stimulation. A previous study demonstrated that periodically turning on and off sinusoidal magnetic stimulations could actually improve triggered release rates compared to continuous sinusoidal magnetic stimulation.[24] Here, this principle was investigated further by adjusting parameters associated with pulsing the magnetic stimulation regiment. Namely, ferrogel inner compartments were exposed to pulsed magnetic stimulation regiments where the frequency and duration of magnetic stimulation pulses were changed vs. time.

It was demonstrated that applying different pulsed magnetic stimulation regiments could be used to control the rate of protein release during magnetic stimulation. For

example, after 3 days of diffusive release, ferrogels containing HSP27 were magnetically stimulated using one of two different pulsed regiments: either a regiment switching between (i) 10 minutes of magnetic stimulation at 5 Hz followed by 50 minutes at 1 Hz, repeated over 4 hours (Figure 6.A.i: Mag-a), or (ii) 10 minutes stimulation at 10 Hz followed by 20 minutes at 2 Hz, repeated over 4 hours (Figure 6. A.i: Mag-b). These two pulsed stimulation profiles resulted in statistically higher release rates on day 3 compared to controls (Figure 6. A. ii and iii). While these two pulsed stimulation profiles produced slightly different stimulated release rates on day 3 from each other, there was no statistically significant difference between them (Figure 6. A. iii: comparing Mag-a to Mag-b release rates). Statistical differences may be achieved in future studies by fine-tuning the material makeup of the ferrogel as well and the magnetic stimulation profile (e.g., different frequencies at different times for different durations and different magnetic field intensities).

The use of different pulsed magnetic stimulation regiments was more effective in regulating the rate of PDGF release. For example, PDGF-loaded inner compartment ferrogels were magnetically stimulated on day 3 using either a pulsed regiment that switched between (i) 10 minutes of magnetic stimulation at 5 Hz followed by 50 minutes at 1 Hz, repeated over 4 hours (Figure 6.B.i: Mag-a), or (ii) 30 minutes stimulation at 5 Hz followed by 30 minutes at 10 Hz, repeated over 4 hours (Figure 6. B.i: Mag-b). Results indicated that both pulsed stimulation profiles enhanced PDGF release rates on day 3 compared to controls (Figure 6.B. ii and iii). Additionally, one magnetic stimulation profile enhanced release rates compared to the other stimulation profile (Figure 6.B. iii: Mag-a is statistically higher than Mag-b).

Based on the differences in magnetically stimulated release rates between HSP27 and BMP2, it is apparent that different proteins have different stimulated release characteristics and that these differences are likely influenced by the interactions between the proteins and the ferrogel's alginate matrices. For example, BMP2 interacts highly with alginate (i.e., BMP2 is heparin-binding and alginate is heparin-mimicking). In fact, when loaded with BMP2, these inner compartment ferrogels had difficulty in releasing BMP2 at rates that were statistically different than controls. For instance, when loaded with BMP2 and stimulated on day 3 using either a pulsed regiment that switched between (i) 10 minutes of magnetic stimulation at 5 Hz followed by 50 minutes at 1 Hz, repeated over 4 hours (Figure 6.C.i: Mag-a), or (ii) 10 minutes stimulation at 14 Hz followed by 20 minutes at 2 Hz, repeated over 4 hours (Figure 6. c.i: Mag-b), the were no observed differences in BMP2 release rates compared to controls (Figure 6.C. ii and iii). Again, however, it may be possible in future studies to demonstrate magnetically triggered releases rates that are statistically higher than controls when optimizing the material makeup of the ferrogel and the magnetic stimulation profile (e.g., different frequencies at different times for different durations and different magnetic field intensities).

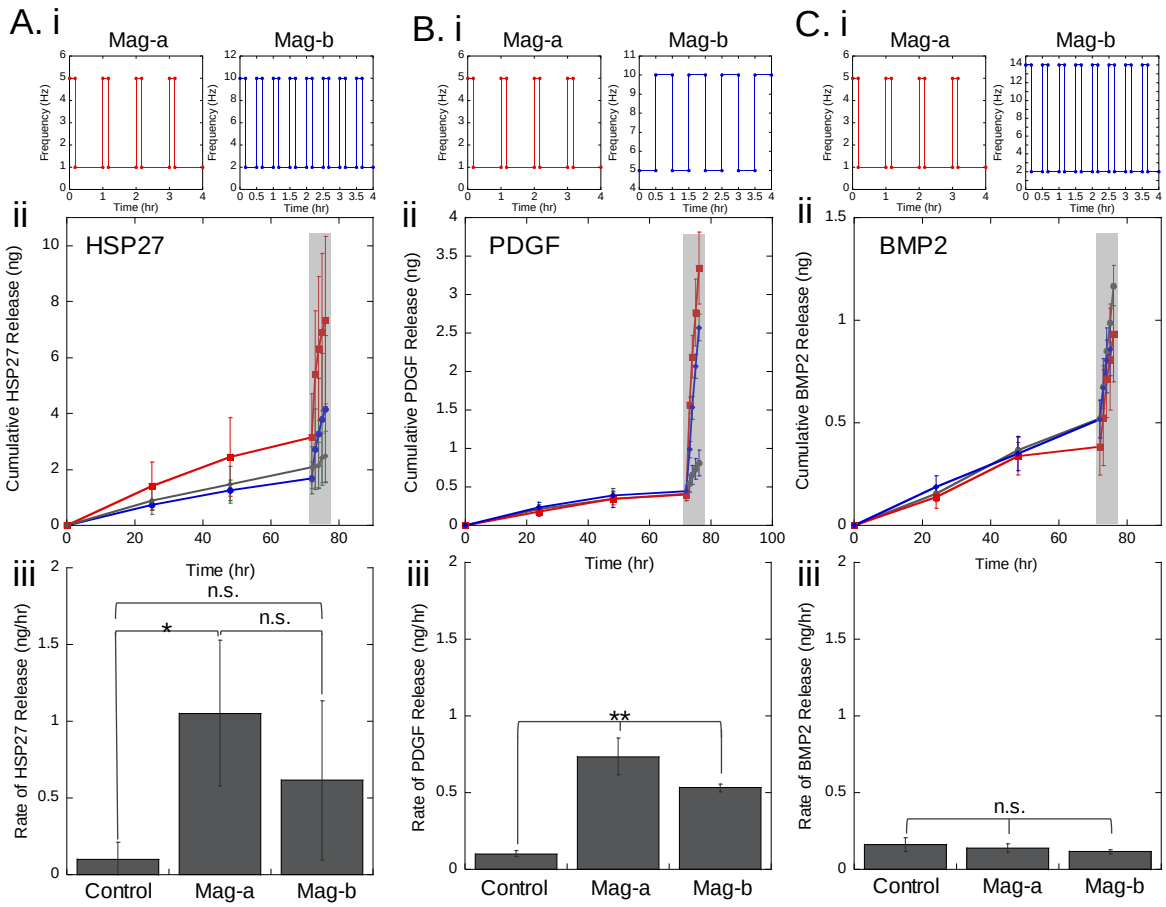

Figure 0.6. Rate of the delivery of proteins from ferrogels can be controlled by applying various frequencies. A,B,C. i) Illustration of the magnetic stimulation used. A,B,C. ii) Cumulative release versus time for HSP27 when not stimulated (grey when stimulated with magnetic profile-a (red) and magnetic profile-b (blue) A,B,C. iii) Release rate from 72 to 76 hours for gels stimulated with nothing, magnetic profile-a and magnetic profile-b.

4.5 Discussion

These two-compartment biomaterial systems may provide improvements in a wide range of biomedical applications, including biomaterial-based cancer immunotherapies, therapies involving regeneration of vascular networks, and in bone regeneration. For example, the sequential deliveries of DC recruitment factors followed

by flexibly timed and delayed delivery of cancer antigen may enable specific improvements in biomaterial-based cancer immunotherapies. While biomaterial-based cancer immunotherapy has shown promising results (90% mouse survival after 3 months after being challenged with xerographic melanoma if biomaterial cancer vaccines were implanted 14 days prior to cancer challenge),[25] when the biomaterial vaccine was implanted in mice with existing melanomas (well-developed 13-day-old tumors) mouse survival rates were less promising.[26] A potential area of improvement for these strategies lies in the timing of DC recruitment and the presentation of cancer antigen to recruited DCs. In the biomaterial melanoma vaccine described above,[25,26] DCs are presented with activation factors (cancer antigen and danger signal) as they enter the scaffold. This may result in (i) diffusive loss of activation factors while DCs are in transient during recruitment and (ii) activation of DCs being distributed over time (i.e., not all DCs arrive in the scaffold and are presented with activation factors at the same time). Both of these may result in a less intense anti-tumor response from the host. The two-compartment magnetically responsive biomaterial system presented could enable recruitment of DCs to the outer compartment and then delivery of activation factors to recruited DCs only after a strong population of DCs has been recruited to the scaffold. In this manner, a strong population of DCs can be activated, enabling a high number of activated DCs to home to the lymph nodes, initiating a potent anti-cancer immunogenic response. Moreover, the biomaterial system described here could enable (i) optimizations in regard to the timing of recruited DC activation and (ii) could provide repeated/subsequent release of activation factors through subsequent magnetic stimulations (i.e., injection-less boosters).

The biomaterial system described here may also provide improvements for therapies where new vasculature needs to be developed. Due to the biology outlined in Fig 1.B, sequential release of pro-angiogenic (VEGF) and pro-maturation (PDGF) factors is necessary for growth of new vasculature. In light of this, Richardson et al.[27] created a biomaterial capable of delivering both VEGF and PDGF, ostensibly in sequence, by composing a scaffold with different degradation rates. While delivery of PDGF alone improved vessel maturation (as measured by the distribution in vessel diameter) compared to VEGF delivery alone, combined release of VEGF + PDGF did not improve average vessel diameter with statistical significance over PDGF delivery alone. This may have been due to the specific temporal profiles of VEGF and PDGF delivery from the system. The differential degradation approach adopted by Richardson et al. yielded VEGF and PDGF release profiles that were more of different rates as opposed to sequential per se. That is, there was not a drastic (albeit slight) increase in PDGF release at later time points (i.e., dramatically delayed PDGF increases in release rate, as observed here in using magnetically responsive ferrogels). This lack of sequential delivery may have not property coordinated the sequence of pericyte detachment, vascular sprouting, vascular invasion, pericyte re-recruitment and attachment, and sprout maturation required to generate mature vasculature. The delivery profiles achieved by the two-compartment biomaterial system described here may more properly coordinate these sequential biological events. Furthermore, the on-demand capabilities of this two-compartment system may enable critical optimization in the timing allowed for sprouting and sprout infiltration prior to initiating vascular maturation.

Finally, the two-compartment magnetically responsive biomaterial system described here might be beneficial for optimizing deliveries in treating bone defects, injuries, and diseases. Regenerating bone requires coordinated sequence recruitment, proliferation, and differentiation events, which can each potentially be coordinated through protein deliveries. In an attempt to coordinate these events, Lee et al.[28] developed a biomaterial that contained two factors with the goal of enhancing the number of calcium phosphate matrix-producing osteoblasts: TGFβ (to enhance the population of bone progenitors resident in the regenerative scaffold) and BMP2 (to differentiate those bone progenitors into osteoblasts). While this strategy demonstrated that BMP2-loaded scaffolds yielded significantly higher amounts of bone-matrix than controls, dual-loaded BMP2/TGFβ scaffolds did not produce more bone matrix than only BMP2-loaded scaffolds (and may in fact have yielded *less* bone matrix). Again, this result may have been due to the timing of how and when these proteins were presented to bone progenitors as they entered the scaffold from surrounding tissues. For example, while TGFβ is known to enhance cell proliferation, it is also known that differentiated cells do not proliferate well.[28] Thus, if cells are instructed to osteo-differentiate by being presented with BMP-2 upon entering the scaffold, they may not proliferate well despite receiving instruction to proliferate through TGFβ presentation. This set of simultaneous and conflicting instructions may have limited the number of osteo-differentiate cells in the Lee et al. studies. However, if presented in sequence (i.e., first to proliferate to a strong population while retaining their stem-like ability to proliferate through TGFβ signaling; and then to differentiate down the osteogenic lineage through BMP2 signaling), it may be possible to generate a more robust population of bone-matrix-

producing osteoblasts. The dual-compartment material system presented here may afford coordination of this sequence and furthermore be capable of optimizing the timing of this sequence for maximized bone matrix production.

4.6 Conclusions

In this study, a biomaterial system was developed and its ability to sequentially release two different proteins pertinent to three therapies was demonstrated. This system was capable of rapidly releasing initial factors (GM-CSF, VEGF, or SDF-1a) from a porous gelatin outer compartment that was designed to facilitate cell infiltration. The amount of this delivery depended on the amount of the factor that was loaded into the outer compartment. Additionally, this biomaterial system contained a magnetically responsive ferrogel inner compartment, which was able to produce enhanced delivery of its payload (HSP27, PDGF, or BMP2) at a time dictated by an externally applied magnetic signal. It was also demonstrated that the rates of these delayed and magnetically triggered protein deliveries could potential be regulated by altering the frequencies and/or temporal profile of the magnetic stimulation itself.

4.7 Acknowledgments

This research was funded by a Medical Research Grant from the Rhode Island Foundation (20144262), an Early Career Development Award from the Rhode Island IDeA Network of Biomedical Research Excellence (RI-INBRE, NIH/NIGMS 2P20GM103430), a 3M Company Non-Tenure Faculty Award (32976949), and a grant from the National Science Foundation (NSF-CBET 1063433). The authors would like to thank Irene Andreu at the RI consortium for Nanoscience & Nanotechnology for help with SEM imaging.

4.8 References

1. Gombotz WR, Pettit DK. Biodegradable Polymers for Protein and Peptide Drug Delivery. 1995;345(206):332-351. doi:10.1021/bc00034a002
2. Kearney CJ, Mooney DJ. Macroscale delivery systems for molecular and cellular payloads. *Nat Mater*. 2013;12(11):1004-1017. doi:10.1038/nmat3758
3. Singh A, Peppas NA. Hydrogels and scaffolds for immunomodulation. *Adv Mater*. 2014;26(38):6530-6541. doi:10.1002/adma.201402105
4. Facts C. Cancer Facts & Figures 2017. 2017.
5. Klinman DM. Immunotherapeutic uses of CpG oligodeoxynucleotides. *Nat Rev Immunol*. 2004;4(4):249-259. http://dx.doi.org/10.1038/nri1329.
6. Li WA, Mooney DJ. Materials based tumor immunotherapy vaccines. *Curr Opin Immunol*. 2013;25(2):238-245. doi:10.1016/j.coi.2012.12.008
7. Kim J, Mooney DJ. In vivo modulation of dendritic cells by engineered materials: Towards new cancer vaccines. *Nano Today*. 2011;6(5):466-477. doi:10.1016/j.nantod.2011.08.005
8. Kochanek KD, Murphy SL, Xu J. National Vital Statistics Reports Deaths : Final Data for 2014. 2017;65(4).
9. Kottke TE, Giles WH, Capewell S. Explaining the Decrease in U.S. Deaths from Coronary Disease, 1980–2000. 2007:2388-2398.
10. Werner S, Grose R. Regulation of wound healing by growth factors and cytokines. *Physiol Rev*. 2003;83(3):835-870. doi:10.1152/physrev.00031.2002
11. Eming SA, Martin P, Tomic-canic M, Park H, Medicine R. Wound repair and

regeneration: Mechanisms, signaling, and translation. *Sci Transl Med*. 2016;6(265):1-36. doi:10.1126/scitranslmed.3009337.Wound

12. Henkel J, Woodruff MA, Epari DR, et al. Bone Regeneration Based on Tissue Engineering Conceptions – A 21st Century Perspective. *Nat Publ Gr*. 2013;1(3):216-248. doi:10.4248/BR201303002

13. Lee KY, Peters MC, Anderson KW, Mooney DJ. Controlled growth factor release from synthetic extracellular matrices. *Nature*. 2000;408(6815):998-1000. doi:10.1038/35050141

14. Services H. Bone Health and Osteoporosis A Report of the Surgeon General.

15. Boyan BD, Baker MI, Lee CSD, Raines AL. *Bone Tissue Grafting and Tissue Engineering Concepts*. Elsevier Ltd.; 2011. doi:10.1016/B978-0-08-055294-1.00167-7

16. Younger EM, Chapman MW. Morbidity at bone graft donor sites. 1989;(January 1982):3-5.

17. Mehta M, Schmidt-bleek K, Duda GN, Mooney DJ. Biomaterial delivery of morphogens to mimic the natural healing cascade in bone ☆. *Adv Drug Deliv Rev*. 2012;64(12):1257-1276. doi:10.1016/j.addr.2012.05.006

18. Ennett AB, Kaigler D, Mooney DJ. Temporally regulated delivery of VEGF in vitro and in vivo. 2006. doi:10.1002/jbm.a

19. Chen F, Chen R, Wang X, Sun H, Wu Z. Biomaterials In vitro cellular responses to scaffolds containing two microencapulated growth factors. *Biomaterials*. 2009;30(28):5215-5224. doi:10.1016/j.biomaterials.2009.06.009

20. Dual delivery of an angiogenic and an osteogenic growth factor for bone

regeneration in a critical size defect model. *Bone*. 2008;43(5):931-940. doi:10.1016/J.BONE.2008.06.019

21. Cezar C a, Kennedy SM, Mehta M, et al. Biphasic Ferrogels for Triggered Drug and Cell Delivery. *Adv Healthc Mater*. 2014:1-8. doi:10.1002/adhm.201400095
22. Kennedy S, Roco C, Déléris A, et al. Improved magnetic regulation of delivery profiles from ferrogels. *Biomaterials*. 2018;161:179-189. doi:10.1016/j.biomaterials.2018.01.049
23. Emi T, Barnes T, Orton E, et al. Pulsatile Chemotherapeutic Delivery Profiles Using Magnetically Responsive Hydrogels. *ACS Biomater Sci Eng*. 2018. doi:10.1021/acsbiomaterials.8b00348
24. Tolouei AE, Dülger N, Ghatee R, Kennedy S. A Magnetically Responsive Biomaterial System for Flexibly Regulating the Duration between Pro- and Anti-Inflammatory Cytokine Deliveries. *Adv Healthc Mater*. 2018;7(12). doi:10.1002/adhm.201800227
25. Ali O a, Huebsch N, Cao L, Dranoff G, Mooney DJ. Infection-mimicking materials to program dendritic cells in situ. *Nat Mater*. 2009;8(2):151-158. doi:10.1038/nmat2357
26. Ali O a, Emerich D, Dranoff G, Mooney DJ. In situ regulation of DC subsets and T cells mediates tumor regression in mice. *Sci Transl Med*. 2009;1(8):8ra19. doi:10.1126/scitranslmed.3000359
27. Richardson TP, Peters MC, Ennett a B, Mooney DJ. Polymeric system for dual growth factor delivery. *Nat Biotechnol*. 2001;19(11):1029-1034. doi:10.1038/nbt1101-1029

28. Lee K, Weir MD, Lippens E, et al. Bone regeneration via novel macroporous CPC scaffolds in critical-sized cranial defects in rats. *Dent Mater*. 2014;30(7):e199-e207. doi:10.1016/j.dental.2014.03.008

Chapter 5

Summary and Prospective Research

5.1 Primary goals

The research described in this dissertation was to investigate magnetically responsive drug delivery systems and develop a biomaterial system capable of controlling the rate and timing of different biomolecular deliveries in response to a remotely applied magnetic fields. More specifically, this doctoral research aimed to (1) develop a dual compartment biomaterial system capable of generating sequences of biomolecular deliveries in response to low-frequency, spatially graded magnetic fields, and (2) to investigate the applications of this developed biomaterial for delivering critical biomolecules in several therapeutic applications that may be enhanced through sequential deliveries.

5.2 Summary of individual chapters

While Chapter 1 broadly motivated the work that is contained in this dissertation, Chapter 2 elaborated on this motivation by discussing existing hydrogel-based magnetically responsive biomaterials with some highlighted examples and in terms of mechanisms of magnetically triggered release and parameters that influence release characteristics. A few case studies were examined where magnetically responsive

hydrogels were used to generate temporally complex and multi-drug delivery profiles. However, Chapter 2 in fact underscored how not many magnetically responsive biomaterials had been introduced that demonstrated the capability of regulating temporally complex, multi-drug deliveries. This underscores the urgency for novel biomaterial systems with these capabilities. Thus, in Chapters 3 and 4, a novel biomaterial system was described that was specifically designed to generate temporally complex, multi-drug delivery profiles in response to remotely applied magnetic stimuli.

Chapter 3 focused on developing and demonstrating novel delivery capabilities for a biomaterial system possibly capable of regulating the inflammation response in wound healing applications. This two-compartment biomaterial system was designed to initially release factors that could recruit a population of pro-inflammatory macrophages (i.e., by delivering MCP-1 and IFNg from an outer compartment that was porous and presented integrins for macrophage binding). Magnetically triggered release of anti-inflammatory factors (i.e., IL4 and/or IL10 from a magnetically deformable ferrogel as the inner compartment) was designed to switch off the inflammation and the promote healing processes.

Chapter 4 explored the use of this two-compartment biomaterial system in additional applications where remote regulation of the timing of sequential biomolecular deliveries may be of high clinical value. Specifically, the dual compartment biomaterial system was loaded with biomolecules pertinent to cancer immunotherapy, tissue vascularization, and bone regeneration. Biological processes relevant to these three applications can each benefit sequential regulation of biosocial events through sequenced biomolecular deliveries. For instance, in biomaterial-based cancer immunotherapy

applications, a goal for potentially improving these therapies is to increase the number of the activated dendritic cells. This possibly can be done by releasing DC recruitment factor while holding on to the activating factor inside the ferrogel and have it be released to recruited DCs only when the DC population is relatively high. This would lead to increased numbers of activated immune cells and a stronger anti-cancer immune response. Indeed, the two-compartment biomaterial system developed was demonstrated to sequentially deliver DC recruitment factors (i.e., GM-CSF) followed by magnetically triggered delivery of DC activation factors (i.e., single stranded DNA and a model protein antigen, HSP-27). In tissue vascularization applications, the aim was to demonstrate sequential deliveries that could direct the sprouting of immature vascular sprouts, followed by coordination of events that lead to maturation of those vascular sprouts. Indeed, the two-compartment biomaterial system was demonstrated to sequentially deliver pro-angiogenic sprouting factors (i.e., VEGF) followed by magnetically triggered pro-maturation factors (i.e., PDGF). In bone regeneration applications, the aim was to demonstrate sequential deliveries that could first recruit bone progenitor cells followed by differentiation of those recruited progenitor cells down the osteogenic lineage. Again, this work successfully demonstrated the ability to first release a bone progenitor recruitment factor (SDF-1a) followed by magnetically triggered release of an osteo-differentiation factor (BMP-2).

5.3 Impact and importance of this work

The biomaterial system developed and demonstrate in this dissertation can potentially be used to help scientists better understand how the dosing, sequence, and timing of the drug release can impact the outcome in wound healing, cancer

immunotherapies, and tissue engineering (i.e., neo-vascularization of and establishing populations of tissue-specific cell types within defect sites). This can help scientists optimize different drug delivery regiments before moving on to clinical trials and implementing the dosing on patients. Also, the on-demand nature of these magnetically responsive materials will help enable rapid optimizations since the material itself does not need to be altered between experiments (i.e., the same material system is capable of producing a wide variety of delivery profiles whereas a traditional biomaterial must be reformulated to produce different delivery profiles). Furthermore, the on-demand nature of these magnetically responsive biomaterials would enable real-time alterations in delivery schedules, which would provide a high degree of flexibility for clinicians to alter the course of therapy in real time according to updates in patient prognosis. Finally, from a practical standpoint, the magnetic stimulations needed for these triggered deliveries involve benign fields from simple, inexpensive, hand-held magnets.

Another significant aspect of this project involves the fact that this developed drug delivery system can be made with variety of biomaterials in different shapes and sizes and can be loaded with many different bioactive molecules, depending on the desired application. For example, the porosity of the outer compartment can be adjusted for controlling the diffusion rate of the drug as well as the chemistry of the polymer which can be easily modified to attach different molecules to it. Also, these biomaterials can be designed to degrade in body within a desired timeframe, which holds up the need to take out the biomaterial once it is no longer required. This is particularly desirable in tissue engineering applications where the body will replace the scaffold with its own native extracellular matrix.

5.4 Future directions

While some very critical developments, characterizations, and demonstrations were performed in this dissertation, the biomaterial system developed here needs to be further examined in vitro and in vivo in order to truly uncover its ability to therapeutically regulate key biological processes. For example, for demonstrating the use of the dual compartment system in controlling macrophage phenotype change vs. time in vitro, RAW 264.7 (ATCC(R) TIB-71™) could be seeded in 12 well plates. The dual compartment biomaterial system would be loaded with factors so that M1 (inflammatory) macrophages would be rapidly recruited to the outer compartment. Factors that could transition those M1 macrophages into pro-healing (anti-inflammatory) M2 macrophages would be loaded in the inner compartment (where they would remain until magnetically triggered to release). This loaded biomaterial would be placed on top of the seeded macrophages and they would be allowed to infiltrate the outer compartment where they would establish a population of M1 macrophages. Over the course of several days, the biomaterial could be magnetically stimulated at different times, releasing anti-inflammatory factors (IL4 and/or IL10) to trigger an anti-inflammatory response in the macrophages (i.e., transition them from M1 to M2 phenotypes) at different times. The phenotype of macrophages resident in the biomaterial can be quantified vs. time by using common antibody staining (anti-mouse CCR7 for M1 macrophages and anti-mouse CD206 for M2) or by measuring the proteins secreted by macrophages (VEGF for M1 macrophages and PDGF for M2 macrophages). In this manner, the biomaterials system's ability to regulate macrophage phenotype vs. time can be tested/verified.

For testing its application in cancer immunotherapy, JAWSII (ATCC® CRL-11904™) that are immature dendritic cells (DCs) could be seeded in 12 well plates. Biomaterial system can be loaded with DC recruitment factor in the outer compartment and DC activating factor in the inner ferrogel. The dual compartment system then can be placed on top of the seeded dendritic cells. With release of the recruitment factor from the outer compartment (GM-CSF), DC cells will populate the gelatin part of the system, after few days ferrogel can be triggered to release activating factors such as cancer antigen (i.e., Heat shock protein 27 (HSP27) or danger signal, single stranded nucleic acid (ssNA)). Activation of the dendritic cells can be validated by antibody staining the cells for both "anti-mouse CCR7" and "anti-mouse MHCII" marker on the cells. We can collect the histogram for stained cells using Nexcelom cellometer. Also cell studies need to be done in regulating sprouting and pericyte/endothelial cell co-localization in vascular models. A co-culture of independently stained endothelial cells (red) and pericytes (blue) is required. In order to do that we plan on seeding the Human dermal microvascular endothelial cells (HMVECs) that are stained with octadecyl rhodamine B chloride, (R18, Molecular Probes O-246-blue) along with Pericytes stained with CMFDA (red). These two cell lines will be co-cultured on a fibrin laden 6-well plate. Biomaterial system will be placed on top of the culture with media. Diffusive release of VEGF from the gelatin triggers pericyte detachment and forming of the vessel sprouts. The stimulated PDGF release helps pericyte attachment and initiates vessel maturation. The number of vessel sprouts and number of attached and detached pericytes will be manually counted using confocal microscopy technique. Moreover, for in vitro model in improving oseto-differentiation in bone regeneration, mesenchymal stem cells (MSCs) can be seeded in

well plates. Dual compartment system loaded with stromal cell derived factor 1 (SDF-1α) in outer section for recruiting MSCs and bone morphogenetic protein-2 (BMP-2) loaded inner ferrogel can be placed on top of the cells. After stem cell recruitment to the biomaterial, stimulated release of BMP-2 from the ferrogel will differentiate the MSCs to bone lineage. For counting the recruited cells, we can fix and stain the gel holding the cells with DAPI for cell nuclei and Phalloidin to stain the F-actin and images were taken using confocal microscope. For osteo-differentiation, the culture media can be collected on daily basis and analyzed using ELISA for "osteocalcin" secretion as indicator of early stage osteo-differentiation and for "Alizarin Red" to stain calcium phosphate as an indicator of late stage osteo-differentiation.

Appendix A

Supporting Information

for *Adv. Healthcare Mater.*, DOI: 10.1002/adhm.201300260

A Magnetically Responsive Biomaterial System for Flexibly Regulating the Duration Between Pro- and Anti-Inflammatory Cytokine Deliveries

By Anita E. Tolouei, Nihan Dülger, Rosa Ghatee, Stephen Kennedy[*]

Materials: Sodium alginate was donated from Pronova Biopolymers (Oslo, Norway) with an average molecular weight of ~250 kDa and with high guluronate content (Protoanal LF 20/40). Adipic acid dihydrazide (AAD), 1-ethyl-3-(dimethylaminopropyl) carbodiimide (EDC), MES, 1-hydroxybenzotriazole (HOBT), iron (II,III) oxide powder (< 5 micron), Phosphate Buffered Saline (PBS), Sigmacote®, bovine serum albumin (BSA), paraformaldehyde (PFA), Triton X-100, fluorescein isothiocyanate (FITC) labeled phalloidin, and 2-(4-Amidinophenryl)-6-indolecarbamidine dihydrochloride (DAPI) were all purchased from Sigma-Aldrich (St. Louis, MO). Mouse Monocyte Chemoattractant Protein-1 (MCP-1), Interferon Gamma (IFN-γ), Interleukin-4 (IL-4), Interleukin-10 (IL-10), and all Enzyme-linked Immunosorbent Assay (ELISA) kits and kit reagents were purchased from R&D Systems (Minneapolis, MN).

Macrophage culturing: RAW 264.7 mouse macrophages (ATCC, Manassas, VA) were used in these studies. Macrophages were cultured in Dulbecco's Modified Eagle's Medium (DMEM, Sigma) containing 10% fetal bovine serum (FBS, Sigma) and 1% penicillin-streptomycin (Sigma) in 75 cm^2 flasks at 37ºC and 5% CO_2 and split every 2-3

days at a 1:3 to 1:6 ratio, as recommended by the manufacturer.

Mechanical characterization of biphasic ferrogels before and after magnetic stimulation: Biphasic ferrogel (inner compartments) stiffness (Young's modulus) before and after magnetic stimulation was quantitatively measured in compression using an Instron Model 3345 (Norwood, MA). Prior to magnetic stimulation, biphasic ferrogels were placed between the plates of the Instron and compressed (at 2 mm/min) until reaching 50% strain in order to produce a well-define elastic region on the stress-strain curve. Note that this compression resulted in deformation of only the iron-oxide-free region of the ferrogels and not the much stiffer/denser iron-oxide-laden region. Recorded stress-strain curves were analyzed using the Instron's Bluehill software package to extract moduli. Because this compression test could have damaged the gels, separate sets of gels were magnetically stimulated and mechanically tested after being exposed to magnetic stimulation profiles.

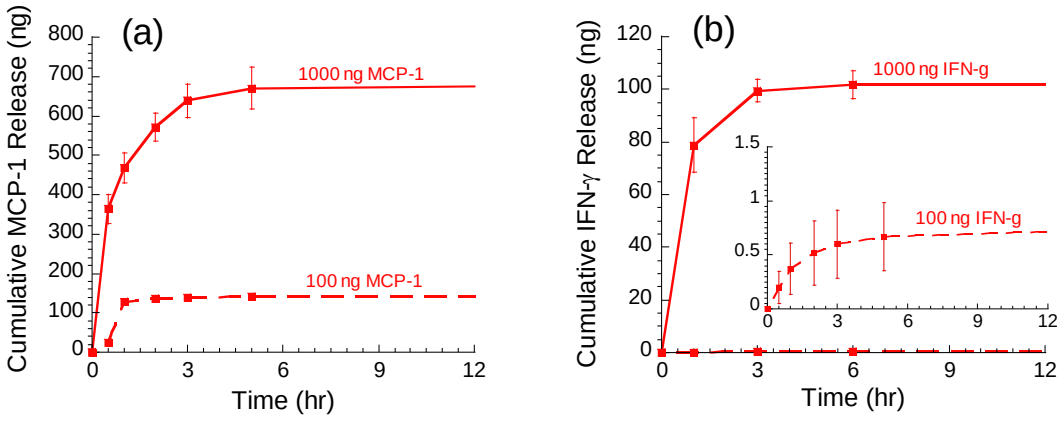

Figure 0.1. S1. Outer porous gelatin scaffolds rapidly released MCP-1 and IFN-γ in the first 12 hours. (a) Cumulative MCP-1 release during the first 12-hours of experimentation for gelatin scaffolds loaded with 1000 ng (solid red) and 100 ng (dashed red) MCP-1. (b) Cumulative IFN-γ release during the first 12-hours of experimentation for gelatin scaffolds loaded with 1000 ng (solid red) and 100 ng (dashed red) IFN-γ. Inset: zoom-in of cumulative release for 100 ng-loaded scaffolds. For parts (a) and (b), N = 4.

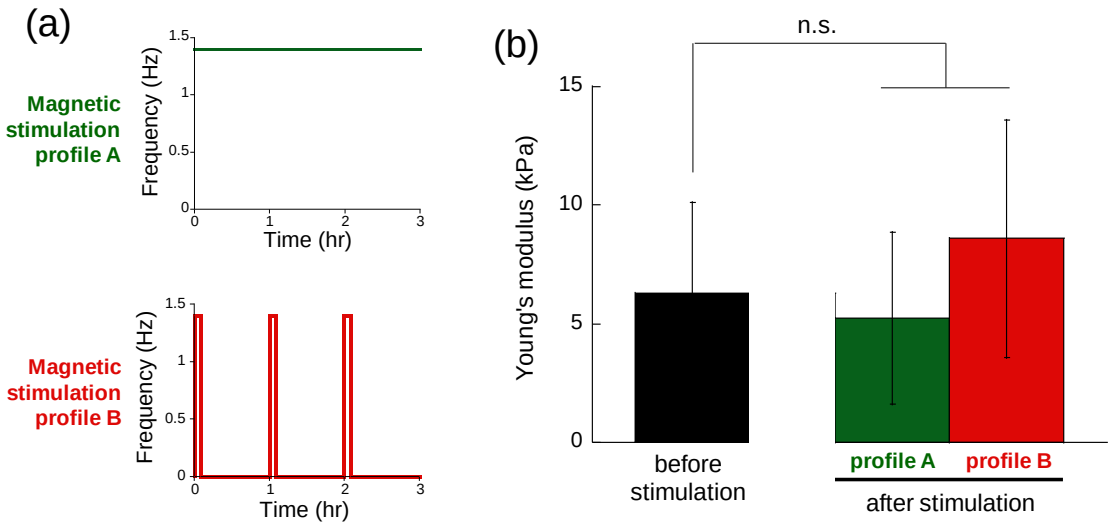

Figure 0.2. S2. Ferrogel mechanics did not significantly change due to magnetic stimulation. (a) Schematics of the two stimulation profiles used: continuous stimulation at 1.4 Hz for 3 hours (top) and periodic stimulation at 1.4 Hz for 5 min every hour on the hour for 3 hours. (b) Young's modulus of ferrogels before stimulation (black), after stimulation profile A (green), and after stimulation profile B (red). N = 4.

<< MovieS1.avi >>

Movie S1. 3D z-stack reconstruction of macrophages recruited to the bottom 170 μm of a porous gelatin scaffold. Scaffold and macrophages were stained to identify f-actin (green) and cell nuclei (blue).

<< MovieS2.mov >>

Movie S2. Biphasic ferrogel being cyclically compressed at 1.4 Hz using a magnet on our custom rocker setup.